Baroclinic energy conversion as driver for Rossby wave breaking

W. Boosman

Utrecht University

Utrecht University

Baroclinic energy conversion as driver for Rossby wave breaking

by

W. Boosman

to obtain the degree of Master of Science
at the Utrecht University.

Student number: 6261051
Project duration: November, 11, 2019 – June 30, 2020
Thesis committee: Dr. A.J. van Delden, Utrecht University, supervisor
Dr. M.L.J. Baatsen, Utrecht University

Utrecht University

List of symbols

θ	–	Potential temperature
Π	–	Potential vorticity
ζ	–	Relative vorticity
σ	–	Isentropic density
$\mathbf{V}$	–	Velocity vector
u	–	Zonal velocity
v	–	Meridional velocity
T	–	Temperature
p	–	Pressure
f	–	Planetary vorticity
ρ	–	Density
M	–	Montgomery streamfunction
Φ	–	Geopotential
Γ	–	Lapse rate
ω	–	Vertical velocity [pressure]
w	–	Vertical velocity
e	–	Efficiency

List of abbreviations

PV	–	Potential Vorticity
RWB	–	Rossby Wave Breaking
AWB	–	Anticyclonic wave breaking
CWB	–	Cyclonic wave breaking
BEC	–	Baroclinic energy conversion
APE	–	Available potential energy
KE	–	Kinetic energy

Preface

I would not be able to write this thesis if it wasn't for some individuals keeping me on track.

Foremost, I would like to thank my enthusiastic supervisor Dr. A.J. van Delden for sharing his atmospheric dynamics expertise with me and showing me interesting scientific areas. I would like to thank him for showing patience and making time for all the questions I had. Even when meeting physically became impossible.

Furthermore, I would like to thank Dr. M.L.J Baatsen. I really enjoyed and appreciated the fact that I could just walk into your office with a single question and that multiple hours later you did not only answer that single question but answered a wide range of questions I didn't even know I had. Your enthusiasm taught me a lot of things.

W. Boosman
Utrecht, July 2020

Abstract

The topic of extreme weather in the mid-latitudes remains a subject of discussion. The response of Rossby waves (and the jetstream that tracks them) to a warming climate is very uncertain, while this large scale flow is known to be the driver for synoptic weather. A comprehensive theory on Rossby wave growth and breaking is hard to determine due to its nonlinear nature. This study advocates for the use of vertical velocity relative to isentropic surfaces to describe the conversion of available potential energy into kinetic energy. It is found that large areas of ***baroclinic energy conversion***(BEC) can be found in the mid-latitudes in the middle as well as the upper troposphere. Intense regions of (BEC) can be found along the meridional moving jetstream in the vicinity of relative vorticity minima and maxima, meaning this could play an important role in amplifying Rossby waves. In an Eulerian frame it is found that regions of BEC coincide with jetstreaks. Results from the Lagrangian framework suggest that BEC might be the energy source of the formation or strengthening of jetstreaks.

Contents

1 Introduction

1.1. Background

In the mid-latitudes winds are predominantly westerly. ***Red skies at night, sailor's delight***[1] is a nice example of a very old saying originating from the new testament emphasizing this is some very old wisdom. These winds grow stronger with height reaching maximum velocities in the upper troposphere. This large scale flow steers the synoptic weather patterns along the so called storm track. These weather patterns in turn steer the jetstream in a meandering pattern (Nakamura and Huang). These jetstream meanders usually move eastward and can be viewed as the Rossby waves. The eastward propagation of these waves cause a varying pattern of weather in the mid-latitudes, eastward moving cyclones make place for anticyclones and vice versa.

However, not all Rossby waves[2] share the same behaviour. Large amplified Rossby waves can bring extreme weather in various forms (Kornhuber et al. (2020)). The case in which the streamlines of large Rossby waves overturn is referred to as Rossby wave breaking (RWB) and can in particular be responsible for extreme weather in the mid-latitudes. Rossby waves can break in a cyclonic tendency (CWB) as well as in an anticyclonic manner (AWB). Cut off lows (COL's) are low pressure systems which are often the product of cyclonic Rossby wave breaking and can bring extreme precipitation (Ndarana and Waugh (2010)). Furthermore, multiple studies found that anticyclonic Rossby wave breaking plays a pronounced role in the onset of blocking anticyclones[3] (e.g. Weijenborg et al. (2012) and Pelly and Hoskins (2003)). Blocking highs are synoptic weather patterns that occur when a Rossby wave persists in the same place relative to the earth and diverges or blocks the westerly mid-latitude jet. Blocking anticyclones can be accompanied with extreme weather, for example, droughts and hot weather in summer, while in winter they can cause severe cold air outbreaks (e.g. Schaller et al. (2018)). Since blocking anticyclones are very slowly moving, they can bring persistent weather for the duration of a couple weeks. In 2018 this has lead for example to the second driest summer in the Netherlands since the start of the measurements. Financial losses are projected to be hundreds of millions, and the effect on the forestry and agriculture can be clearly seen from space.

However, the mechanism behind blocking onset is still topic of debate, and thus blockings are still hard to predict more than 10 days in advance (e.g. Lee et al. (2019a)). Multiple studies try to tackle the formation of blockings from different perspectives, but clear and unambigu-

[1] Red skies are the result of scattered blue light by trapped particles in a stable air mass. The sun sets in the west, so a red sky at night implies that the stable air mass (and thus good weather) are to the west of the observer (the sailor). Since winds are predominantly westerly, this means that fine weather is moving towards the sailor (thus 'sailors delight').

[2] Also known as 'Planetary waves'

[3] Also called 'blocking highs' or even more simple a 'block'

ous conclusions are more the exception than the rule.

Davini et al. (2014) showed that in the Atlantic sector sudden stratospheric warmings (SSW's), are followed by an increased blocking frequency, however the same signal is not found in the Pacific area, so questions about the exact coupling between the stratosphere and troposphere remain unanswered. Lee et al. (2019a) also found a relation between blocking patterns and changes in the strength of the stratospheric polar vortex, however, compared to Davini et al. (2014) they found the cause and effect to be reversed, meaning, the blocking is a precursor to a weaken stratospheric polar vortex.

Studies from tropospheric perspectives focus on moist as well as on dry atmospheric dynamics. A study from Yamazaki Dr. and Itoh 2013 found that blocking anticyclones actively select and absorb synoptic vortices with the same anticyclonic tendency. Other research also focuses on diabatic effects in advance to the onset of a blocking anticyclone, for example, Pfahl et al. (2015) point out the importance of latent heating in the warm conveyor belt as an first order mechanism for the formation and maintenance of the block. They found that latent heat release transports air from lower levels with lower potential vorticity (PV) values into the ridge. This is in line with the findings of Joos and Wernli (2012) which describe this process in a different way, but with the same implications, namely that PV gets destroyed above the the level of maximum heating and increases below the level of maximum heating, and is therefore of great importance.

Despite the uncertainty on the mechanisms behind blocking events, the literature agrees on the fact that blocking anticyclones can have severe weather impacts, such as the drought of 2018 in western Europe. Therefore a good understanding of blocking and the underlying theory (which probably involve Rossby waves) is desirable, mainly for predictions of extreme weather in the near future as temperatures will continue to rise under the influence of anthropogenic climate change. While there is an increase in dry summers observed over the past decades, climate models are modelling a persistent decrease in atmospheric blocking (Woollings et al. 2018). The logical consequence is that there is very low confidence in the future predictions on blocking anticyclones by the IPCC (technical summary, TS.5.4.8).

Looking at extra-tropical cyclones, Papritz and Spengler (2015) see available potential energy as primary source for cyclogenesis. They approach the problem by looking at the slope tendency of the isentropic surfaces. This study proposes a balance between the adiabatic tilting of isentropic surfaces to the horizontal necessary for baroclinic instability and diabatic effects which have an opposite effect and thus restore the background gradient. The study points out that isentropic slopes are a measure for baroclinicty in the mid-latitudes. This is in line with previous work from van Delden and Neggers (2003) which emphasizes the importance of baroclinic energy conversion in cyclogenesis at upper levels. Baroclinic energy conversion (BEC) is the process in which ***available potential energy*** (APE) is lost by lowering the center of mass of the atmosphere, this energy is released as ***kinetic energy*** (KE). The lowering of the center of mass of the atmosphere is driven by baroclinic instability.

The author hypothesises that baroclinic energy conversion is not solely reserved as a diagnostic tool for the explanation of (upper level) cyclogenesis. The author expects that the process is a measure for baroclinicity which is just as important to the onset of blocking anticyclones. Or to put it more broadly, the expectation is that large areas of baroclinic energy conversion are (partly) responsible for accelerating (formation jetstreaks) and thereby steering the jetstream. In this way, baroclinic energy conversion is responsible for the amplification of Rossby waves, which on its turn can have the consequence of extreme weather by the formation of intense extra-tropical cyclones and blocking highs.

1.2. Objective

This study continues on previous work from van Delden and Neggers (2003). Within this study the role of baroclinic energy conversion with respect to Rossby wave amplification is

examined in a new quantitative way. The research will focus on identifying regions where APE can be converted into EKE, and will try to answer the question whether this process does indeed steer and accelerate the jet stream. The sub-questions that are related to this object are:

1. How can the description of baroclinic energy conversion be extended from a qualitative picture into a quantitative one?
2. How does baroclinic energy conversion contribute to Rossby wave amplification (RWB)?
3. What is the role of diabatic processes within baroclinic energy conversion?
4. Can baroclinic energy conversion shine a new light on the ongoing debate of future weather events under the influence of anthropogenic climate change?

1.3. Outline

This thesis will continue with the conceptual explanation of baroclinic energy conversion in chapter 2. Chapter 3 will be concerned with the methodology in which the process of BEC as explained in chapter 2 is described in the real atmosphere using era-5 reanalysis data. Then, chapter 4 will give an introduction to the case study in which the method of chapter 3 is tested. The results and the discussion of their meaning are presented in chapter 5. After the results, chapter 6 discusses the implications of BEC with respect to a warming climate. Chapter 7 will give conclusions of this study and further recommendations.

2

Baroclinic energy conversion and jetstreak formation

This chapter is written to inform the reader on the theory of baroclinic energy conversion. In this chapter it is shown under which conditions the center of mass of the atmosphere can be lowered, in favour of kinetic energy. Section 2.1 will introduce the reader with multiple vertical coordinate systems, and its advantages. This knowledge is necessary to understand the principles of unstable up- and downgliding. The process is described in a conceptual manner with help of a thought experiment in section 2.2. Subsequently, section 2.3 will continue on the thought experiment of section 2.2 by describing not only when baroclinic energy conversion is possible, but also when this process proceeds most efficient.

2.1. Motivation coordinate system

In every three dimensional problem, the choice of the right coordinate system can improve the interpretation of the problem. The most intuitive coordinate system is one in which the vertical axis is measured in the same units of the horizontal axis. In most spatial problems this is in meters, however this is not always the most appropriate way to tackle the problem. The hydrostatic balance (see equation 2.1) gives a distinct balance between gravity and vertical pressure forces and is a good approximation to the vertical dependence of pressure in the atmosphere.

$$\frac{\partial p}{\partial z} = -\rho\, g \tag{2.1}$$

So a clear relation between height and pressure in the vertical column exists. For this reason, instead of height, pressure could also be used as a vertical coordinate. In atmospheric dynamics pressure often has given preference over height, as the momentum balance is far more convenient in pressure coordinates.

For now, let's stick to an absolute height frame. Following Newton's second law, the rate of change in momentum can be described by the net forces acting on an air parcel. When scale analysis is done and only the largest forces are included, the momentum equation in height coordinates looks like equation 2.2.

$$\frac{D\mathbf{V}}{DT} + f\,\mathbf{k}\times\mathbf{V} = -\frac{1}{\rho}\nabla p \tag{2.2}$$

The first term on the l.h.s is the acceleration of the air parcel (or change in momentum), the second term on the l.h.s represents the Coriolis acceleration. The term on the r.h.s is the pressure gradient force. When air parcels do not accelerate from their position there is a balance between the Coriolis acceleration and the pressure gradient force. The resulting velocity

field is known to be the ***geostrophic wind***. In height coordinates, this is where problems start to arise, because the velocity field can only be determined when the density field is known. Or in other words, a given horizontal pressure gradient field gives various velocity fields dependent on density.
Pressure as a vertical coordinate has advantage that density drops out of the momentum equation, as will be shown in the following analysis. Equation 2.3 shows how height and pressure are related.

$$\left(\frac{\partial p}{\partial x}\right)_z = -\left(\frac{\partial p}{\partial z}\right)_x \left(\frac{\partial z}{\partial x}\right)_p \tag{2.3}$$

When the hydrostatic equation (2.1) is substituted in equation 2.3, the equation yields:

$$-\frac{1}{\rho}\left(\frac{\partial p}{\partial x}\right)_z = -g\left(\frac{\partial z}{\partial x}\right)_p = -\left(\frac{\partial \Phi}{\partial x}\right)_p \tag{2.4}$$

Where Φ is a variable known as the ***geopotential***, described by equation 2.5. Changing from a height coordinate to a ***isobaric*** coordinate system gives the clear advantage that density is no longer part of the momentum equations, and is replaced by the gradient in geopotential. The momentum equation described in isobaric coordinates changes therefor to equation 2.6. Geopotential, as can be figured out from equation 2.5, is just the work done to move an air parcel from mean sea level to height z. Since the atmospheric density field is a lot harder to determine compared to geopotential, the velocity field is a lot easier to determine in isobaric coordinates.

$$\Phi = \int_0^z g\, dz \tag{2.5}$$

$$\frac{D\mathbf{V}}{DT} + f\,\mathbf{k}\times\mathbf{V} = -\frac{1}{\rho}\nabla p \tag{2.6}$$

Just as pressure can be used as a vertical coordinate, every quantity which has a dependency on height could potentially be used as a vertical coordinate. One quantity in particular is convenient, namely, the temperature an air parcel would have when it is adiabatic compressed from a given pressure to a reference pressure. This quantity is called the ***potential temperature*** and can be described by equation 2.7. Every air parcel has a unique potential temperature which is conserved following adiabatic motion.

$$\theta = T\,(p_s/p)^{R/c_p} \tag{2.7}$$

Potential temperature is derived form the first law of thermodynamics, and after some derivations, it can be shown that changes in potential temperature are proportional to entropy production (see Holton and Hakim (2013)). Adiabatic motion is per definition under the constraint that entropy is conserved, so for adiabatic motion air parcels are bounded to isentropic surfaces.

Since weather systems with a large temporal and spatial scale are approximated by adiabatic conditions, there are many advantages to use isentropic surfaces to analyse certain atmospheric events. 'Horizontal' flow on an isentropic surface is actually three dimensional and can give a lot of information about the adiabatic vertical motion. Furthermore, static stability is inversely proportional to the pressure difference between isentropic surfaces and parcel trajectories can be accurate and easily calculated if the isentropic velocity field is known.

A relation between the rate of change of temperature with height (***lapse rate***) and the rate of change of potential temperature with height can be described due to the dependency of potential temperature on absolute temperature and compression. Using hydrostatic balance and the ideal gas law the following result is derived:

$$\frac{T}{\theta}\frac{\partial \theta}{\partial z} = \frac{\partial T}{\partial z} + \frac{g}{c_p} \tag{2.8}$$

If potential temperature is constant with respect to height, equation 2.8 reduces to:

$$-\frac{dT}{dz} = \frac{g}{c_p} \equiv \Gamma_d \tag{2.9}$$

Equation 2.9 describes the situation in which the atmospheric temperature decreases with height via the ***dry adiabatic lapse rate*** (Γ_d). In this case the atmosphere is statically neutral, meaning that air parcels which undergo an vertical adiabatic displacement will end up in an environment with equal potential temperature. There is no buoyancy force which accelerates the air parcel to its original or any other position.
On the other hand, when potential temperature is height dependent, the atmospheric lapse rate (Γ) differs form the dry adiabatic lapse rate. Using the definition of the dry adiabatic lapse rate from equation 2.9 and equation 2.8 gives the following relation:

$$\frac{T}{\theta}\frac{\partial \theta}{\partial z} = \Gamma_d - \Gamma \tag{2.10}$$

When the atmospheric lapse rate is smaller then the dry atmospheric lapse rate, potential temperature increases with height. This means that the atmosphere is stably stratified. An air parcel undergoing an upward displacement, will find itself in an environment with higher potential temperature and is therefore negative buoyant. The buoyancy force will accelerate the air parcel to its original position. On the other hand, when the atmospheric lapse rate is larger then the dry atmospheric lapse rate, the potential temperature decreases with height and the atmosphere is statically unstable. Air parcels which undergo small vertical displacements will in this case accelerate even further away from their initial position.
However, on synoptic scales, the atmosphere is always stably stratified and potential temperature will always increase with respect to height. Unstable regions will quickly stabilize by convective overturning Holton and Hakim (2013).

This section was intended to make the distinction between three possible vertical coordinate systems and explain their advantage. The next section will continue with an analysis in the ***isentropic*** coordinate system to explain the idea of unstable up- and downgliding.

2.2. Unstable up- and downgliding

As stated before, vertical motion can be unstable in the sense that available potential energy (APE) can be converted into kinetic energy (KE), a process referred to as baroclinic energy conversion. Baroclinic energy conversion can be possible, as will be shown, when the vertical motion is positive or negative. Unstable ***up***gliding and unstable ***down***gliding is the distinction between these two processes which have the same consequence. This section gives an extensive, but conceptual elaboration on how this process works before going into more quantitative descriptions. Furthermore it aims to answer the question on how the new reanalysis data from ERA-5 helps to give new insights in unstable up- and downgliding.

At first sight it seems not intuitive that upward vertical motion can be associated with lowering the potential energy of the system. However, with potential temperature as the vertical coordinate this process can be made clear. First there will be an explanation on the latitudinal dependency of the surfaces of equal potential temperature (isentropes).

A gradient of the isentropes is of first importance for the mechanism of unstable up- and downgliding. From radiative balance, on average, high latitudes are emitting more energy than receive from the sun. The opposite is happening at latitudes around the equator. The surplus and deficit of energy, which is latitude dependent is one reason for the temperature gradient on earth. It would not come to a surprise that surfaces of equal potential temperature are sloping upwards towards higher latitudes. Remember, potential temperature is the temperature an air parcel has when it is adiabatic compressed from its origin to the reference pressure. For example an air parcel with a potential temperature of 330K at the equator does not have to experience the same compression to reach this temperature compared to an air parcel at higher latitudes for the reason that its absolute temperature is higher already.

Figure 2.1 shows a meridional cross section of the atmosphere to emphasize this point. Isentropes (solid black and highlighted lines in the main figure) are distinctively sloping upwards towards the north in the troposphere. The stratosphere is less subjected to meridional temperature gradients, hence the gradients are less strong.

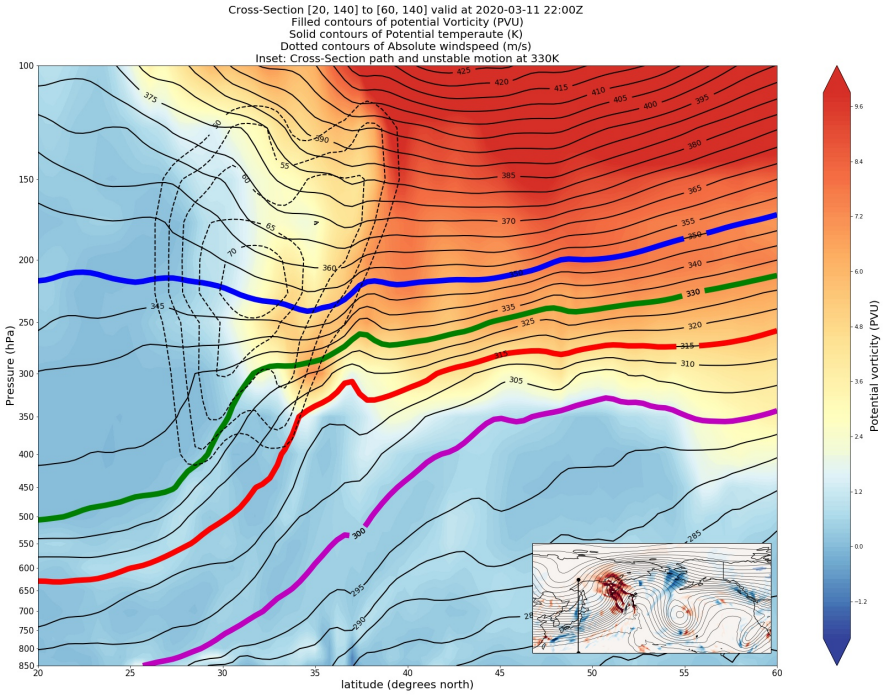

Figure 2.1: Meridional cross section of the atmosphere with solid black and highlighted contours representing surfaces of constant potential temperature. Coloured areas in the main figure represent potential vorticity, with orange colours corresponding to the stratosphere and blue colours to the troposphere. Dashed contours represent absolute wind velocity and the inset figure is meant to illustrate where the cross section is taken.

Following the thought experiment described in Green (1979), unstable up- and downgliding can be described conceptually by exchanging two air parcels with different potential temperature. This is illustrated in figure 2.2. The next part is concerned with the consequences for the potential energy of the system when this exchange is completed.

Following the ideal gas law and the first law of thermodynamics, in adiabatic conditions equation 2.11 has to fulfilled.

$$p_1 {V_1}^{\gamma} = p_2 {V_2}^{\gamma} \tag{2.11}$$

Substituting this relation into the ratio of mass between the two air parcels gives the following relation:

$$\frac{M_2}{M_1} = \frac{\rho_2 V_2}{\rho_1 V_1} = \frac{\rho_2 {p_1}^{1/\gamma}}{\rho_1 {p_2}^{1/\gamma}} \tag{2.12}$$

Substituting the definition of potential temperature (stated in 2.7) into the equation above, the mass ratio can be directly linked to the ratio of potential temperature, which is described in the equation below:

$$\frac{M_2}{M_1} = \frac{\theta_1}{\theta_2} \tag{2.13}$$

With the relation between mass and potential temperature known, the loss of APE can be formulated. In absolute height coordinates the difference of APE after exchanging the two particles from figure 2.2 can be described by the following equation.

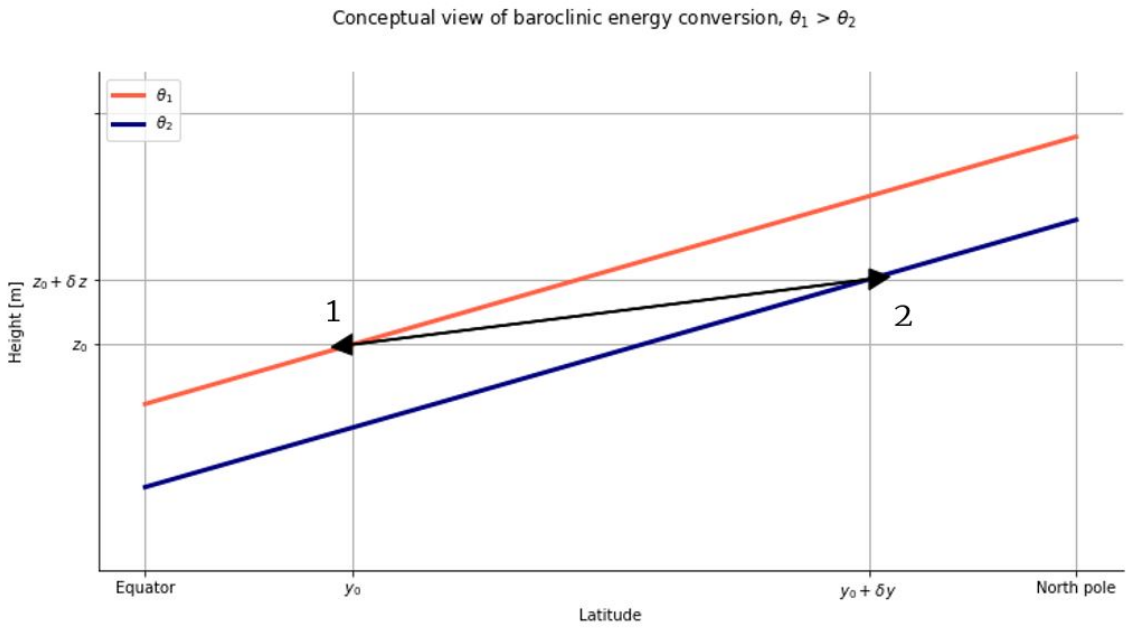

Figure 2.2: A conceptual view of figure 2.1, meant to illustrate the thought experience of Green (Green (1979)), in which air parcel one and two exchange position.

$$\Delta PE = (M_1\, g\, z_2 + M_2\, g\, z_1) - (M_1\, g\, z_1 + M_2\, g\, z_2) = M_1\, g\, (z_1 - z_2) \left(\frac{M_2}{M_1} - 1 \right) \tag{2.14}$$

Substituting equation 2.13 into equation 2.14 relates the change in potential energy to the change in potential temperature through the following relation:

$$\Delta PE = M_1\, g\, (z_1 - z_2) \left(\frac{\theta_1 - \theta_2}{\theta_2} \right) \tag{2.15}$$

In order to convert APE into KE, the left hand side of equation 2.15 has to be smaller then zero. Since the only term on the right hand side of equations 2.15 which can be zero is $(z_1 - z_2)$, the height of air parcel one has to be lower then the height of air parcel two. This is exactly illustrated in figure 2.2.

This criteria corresponds to the definition of ***unstable downgliding*** and ***unstable upgliding***. It should be clear now that APE can be converted into KE when there is vertical motion that can be upward as well as downward. The constraint for motion to be unstable depends on the potential temperature field. From figure 2.2 and the condition for unstable up- and downgliding, it can easily be reasoned that the constraint for the motion to be unstable is that the slope under which the air parcel moves should be ***less*** than the gradient of the isentropes.

2.3. Efficiency

In the previous section the pith of the matter was to define unstable up- and downgliding and explain conceptually the working principle. Motion with slopes less then those of the isentropes have the potential to lower the APE in favour of KE production. However there was no method proposed for the quantification of the energy conversion. This section will proceed with the analysis of unstable up- and downgliding and will give a theory for the quantification for the potential of energy conversion through this mechanism. The theory consists of an analysis for which slope the energy conversion is most favourable.

2.3.1. State of minimal potential energy

The theory for finding the most favorable conditions for energy conversion is based on minimization of the APE. In order to find the state in which the APE in minimum, the trajectory

of two air parcels which exchange position, is expressed in the slope of this trajectory. The slope of the trajectory is described by the angle 'E' which is the angle between the horizontal and the trajectory. The change in potential temperature along this trajectory can also be described by this angle, as is done in equation 2.16. In this equation, 'L' is the length of the trajectory, one could see this as the absolute distance between air parcel one and two in figure 2.2.

$$\theta_2 - \theta_1 = (y_2 - y_1)\frac{\partial\theta}{\partial y} + (z_2 - z_1)\frac{\partial\theta}{\partial z} = \left(\frac{\partial\theta}{\partial y}\cos E + \frac{\partial\theta}{\partial z}\sin E\right) L \tag{2.16}$$

The absolute height difference relates to the slope of the isentropes as follows:

$$z_2 - z_1 = L \sin E \tag{2.17}$$

When equation 2.16 and equation 2.17 are substituted into equation 2.15 the results can be described by the following equation:

$$\Delta PE = \frac{M_1\, g\, L^2}{\theta_2}\sin E\left(\frac{\partial\theta}{\partial y}\cos E + \frac{\partial\theta}{\partial z}\sin E\right) \tag{2.18}$$

In order to find the state in which the energy conversion is maximum, the left hand side of equation 2.18 has to be minimized with respect to variations in 'E'. Taking the derivative of the right hand side and setting it to zero implies:

$$\frac{d}{dE}\left[\sin E\left(\frac{\partial\theta}{\partial y}\cos E + \frac{\partial\theta}{\partial z}\sin E\right)\right] = 0 \tag{2.19}$$

The equation above is satisfied for the condition if :

$$\tan 2E = -\frac{\partial\theta/\partial y}{\partial\theta/\partial z} \tag{2.20}$$

2.3.2. Implications for baroclinic energy conversion

The right hand side of equation 2.20 implies that the maximum amount of APE is destroyed when an air parcel moves along a slope which is half of the gradient of the isentropes in an absolute height coordinate system. This means that large vertical motions which fulfill the conditions for unstable up/- downgliding not necessarily convert large amount of APE into EKE, for example, when the slope of the motion is almost equal to the slope of the isentropes. This deviates from Papritz and Spengler (2015) who only looked at the slope of the isentropes as a measure for cyclogenesis.

This thesis calls for the approach in which there is an efficiency term which is proportional to the slope of the isentropes. A maximum efficiency of one when the motion moves along a slope which is half of the slope of the isentropes, and zero when the slope is the same as the gradient of the isentropes or when the motion is along the horizontal. This gives a more nuanced view on APE to KE conversion associated with baroclinic instability and a more substantiated motivation on the slopes of the isentropic surfaces

This chapter was meant to explain conceptually the principle of unstable up-/ downgliding, however it does not provide any way to determine if and when this phenomena happens in the real atmosphere. The next chapter will go deeper into this problem and provides the reader with the approach how the theory introduced in this chapter is coupled to the ERA-5 reanalysis data.

3
Methodology

The previous chapter is written to define the concept of unstable up- and downgliding and introduce the concept of baroclinic energy conversion. A new approach is proposed to quantify the baroclinic energy conversion through the use of an efficiency term. This chapter will continue on this idea and is written to inform the reader how this idea is applied on real atmospheric data from the ERA-5 reanalysis data-set. The first section will inform the reader on the technical details of the ERA-5 reanalysis data. Section 3.2 will inform the reader on how the supplied data can be transformed to an isentropic coordinate system. The data in the right coordinate system can then be used to identify regions of unstable up- and downgliding. Section 3.3 will be dedicated to this issue. This section will make the translation from the conceptual model from chapter 2 to the analysis of real atmospheric data and also discusses how the efficiency term is determined.

3.1. Supplied data

The supplied data is from the ERA-5 reanalysis dataset from the ECWMF. This dataset has been established by model output which is refined by data assimilation from multiple observation sources. The ERA-5 reanalysis dataset has a spatial resolution of fifteen arcminute and a temporal resolution of one hour. The quantities are given on 27 different pressure levels.

3.2. Isentropic analysis

This section is dedicated to explain how the data given on pressure levels is transformed into data on isentropic levels. The choice of which isentropic levels are meaningful for this study are motivated in subsection 3.2.1. Subsection 3.2.2 describes the technical details on how the data is interpolated from data on isobars to isentropes.

3.2.1. Motivation isentropic levels

As stated above, the supplied data is on pressure levels, and not on isentropic levels. This means that all the data has to be interpolated from pressure levels to isentropic levels in order to comply with the theory given in chapter 2. The chosen isentropic levels to interpolate to are 300K, 315K, 330K and 350K. This choice is motivated by two reasons. At first, the reanalysis data-set available before ERA-5 launched (ERA- Interim) had the option to choose data on an specific isentropic level. The levels of 300K, 315K,330K and 350K were part of the levels one could choose from, therefore, most of the literature which is available and has made use of some kind of isentropic analysis are done on these levels. Secondly, the chosen levels represent certain areas in the atmosphere. The 300K and 315K represents the lower to middle troposphere in the mid-latitudes. This region may not solely be described by adiabatic conditions, since latent heat release may play an important role. Chapter 5 will elaborate on this issue. Higher in the atmosphere lies the isentropic surface of 330K, this level represents the the upper troposphere as well as the lower stratosphere, dependent on latitude and Rossby

wave activity. This is particular useful, for the reason that the stratosphere has very different characteristics compared to the troposphere. Especially, the difference in static stability is remarkable. Adiabatic conditions at the 330K surface form a good approximation, as will be shown later this thesis. Furthermore, the 330K isentropic surface represents the level at which the jetstream approximately lies. The 350K isentropic surface is centered at the lower stratosphere with exception of latitudes lower then ≈ 30° N where this surface may lie in the upper troposphere. Also this level can be approximated by adiabatic conditions.

3.2.2. Isentropic interpolation

Since ERA-5 has no option to download data on surfaces of equal potential temperature, data on pressure levels has to be interpolated to isentropic surfaces. This is possible since potential temperature can be deducted from the the temperature field on pressure levels. For the isentropic interpolation there has been made use of the software package from 'MetPy', which has a function or this interpolation. The interpolation consists of the Newton-Raphson iteration to approximate atmospheric quantities on isentropic surfaces.

3.3. Identify regions of unstable up- and downgliding

The condition for which conversion from APE into KE is established in chapter 2 on the basis of a thought experiment. The condition is matched to either the mechanism of unstable upgliding or unstable downgliding depending on the view of the problem. In the conceptual framework it can easily be seen that the movement of a closed control volume has to occur along a slope less then the gradient of the isentropes to meet these conditions. However finding the vertical motion of air parcels relative to the slope of isentropes may not be trivial. This section is written to inform the reader on how the theory from chapter2 is implemented to real atmospheric data.

3.3.1. Vertical motion in isentropic coordinates

To compare the slope of air parcels relative to the slope of the isentropes, it is of first importance to have a good view on which components make up for the total vertical velocity. This subsection will describe the different components and thus the different processes involved which make up for the total vertical velocity in an isentropic coordinate system. One of the main remarks from section 2.1 was that air parcels move along surfaces of constant potential temperature if they do not undergo diabatic processes. So, in adiabatic conditions, advection on an isentropic surface which is not perfectly horizontal will give rise to vertical velocity. Furthermore, if isentropic surfaces have an instantaneous vertical velocity, this will also give rise to a component in the total vertical velocity because particles are bounded by this surface. The last component which makes up for the total vertical velocity on an isentropic surface are diabatic processes, one could think of latent heat release due to condensation of water vapour in clouds or emission/absorption of radiation. Equation 3.1 summaries the processes described above.

$$\omega = \frac{dp}{dt} = \overbrace{\left(\frac{\partial p_\theta}{\partial t}\right)}^{1} + \overbrace{u\left(\frac{\partial p_\theta}{\partial x}\right)}^{2} + \overbrace{v\left(\frac{\partial p_\theta}{\partial y}\right)}^{3} + \overbrace{\frac{J}{\Pi}\left(\frac{\partial \theta}{\partial p}\right)^{-1}}^{4} \tag{3.1}$$

1. Instantaneous vertical velocity of the isentropic surface
2. Longitudinal advection of isentropic pressure
3. Latitudinal advection of pressure
4. Combined effect of diabatic processes

3.3.2. Necessary conditions

The requirement for baroclinic energy conversion is explained in section 2.2. The main point from this section was that APE can be converted into KE if and only if air parcels move along slopes which are less then the slope of the isentropes. When adiabatic conditions are assumed, equation 3.1 reduces to equation 3.2.

$$\omega = \frac{dp}{dt} = \left(\frac{\partial p_\theta}{\partial t}\right) + u\left(\frac{\partial p_\theta}{\partial x}\right) + v\left(\frac{\partial p_\theta}{\partial y}\right) \tag{3.2}$$

Equation 3.2 can be used to determine if the requirement for baroclinic energy conversion is fulfilled. In order to see this, firstly the combined effect of terms two and three of equation 3.1 will be explained. Terms two and three represent the lift an air parcel experiences when it is advected in a stationary background atmosphere. In other words, the vertical velocity these two terms represent are exactly proportional to the slope of the isentropes.
If terms two and three are proportional to the slope of the isentropes, it should be clear that term one and four are responsible for the vertical velocity relative to the slope of the isentropes. If adiabatic conditions are assumed the fourth term is equal to zero. This means that only the first term can contribute to vertical velocity relative to the gradient of the isentropes. Term one is the instantaneous vertical velocity of the isentropic surface. When this term has the opposite sign compared to the advection term (terms two and three combined), **and** in absolute sense is smaller then the advection term, unstable up- or downglinding can occur.
The following example, illustrated in figure 3.1, will try to clarify the this statement. Assume an air parcel experiencing an upward lift of 2 Pa/s due to advection along a isentropic surface. However, at the same time, this isentropic surface moves downward with an vertical velocity of -1 Pa/s. This means, under adiabatic assumptions, that the total vertical velocity equals 1 Pa/s, while the isentropic gradient would imply a vertical velocity of 2 Pa/s. The gradient under which the air parcel moves **must** be smaller then the gradient of the isentropic surface in this case.

These constraints, necessary for the mechanism of unstable up- and downgliding can be formulated by the following two criteria.

$$\omega > 0 \text{ and } \left(\frac{\partial p_\theta}{\partial t}\right) < 0, \text{ which implies that} \rightarrow \; u\left(\frac{\partial p_\theta}{\partial x}\right) + v\left(\frac{\partial p_\theta}{\partial y}\right) > 0 \tag{3.3}$$

$$\omega < 0 \text{ and } \left(\frac{\partial p_\theta}{\partial t}\right) > 0, \text{ which implies that} \rightarrow \; u\left(\frac{\partial p_\theta}{\partial x}\right) + v\left(\frac{\partial p_\theta}{\partial y}\right) < 0 \tag{3.4}$$

Equation 3.3 and 3.4 give the criteria for unstable down- and upgliding respectively. This result also clarifies the importance of ERA-5 in this study. Results are going to be based on spatial as well as temporal derivatives. Higher spatial and temporal resolution have a direct effect on the precision of the results. Relative to ERA-interim , ERA-5 has a spatial resolution which is ~3 times higher and a temporal resolution which is 6 times higher than ERA-interim.

3.3.3. Efficiency

Section 2.3 tried to make clear that even when criteria 3.4 or 3.3 are satisfied, there is a difference in the amount of APE that get converted into KE dependent on the exact slope relative to the gradient of the isentropes. It was shown that the preferred path is along a gradient which is half relative to gradient of the isentropes. According to subsection 3.3.2, this means that $w\,(= \frac{dz}{dt})$ should be half of $u\left(\frac{\partial z_\theta}{\partial x}\right) + v\left(\frac{\partial z_\theta}{\partial y}\right)$.

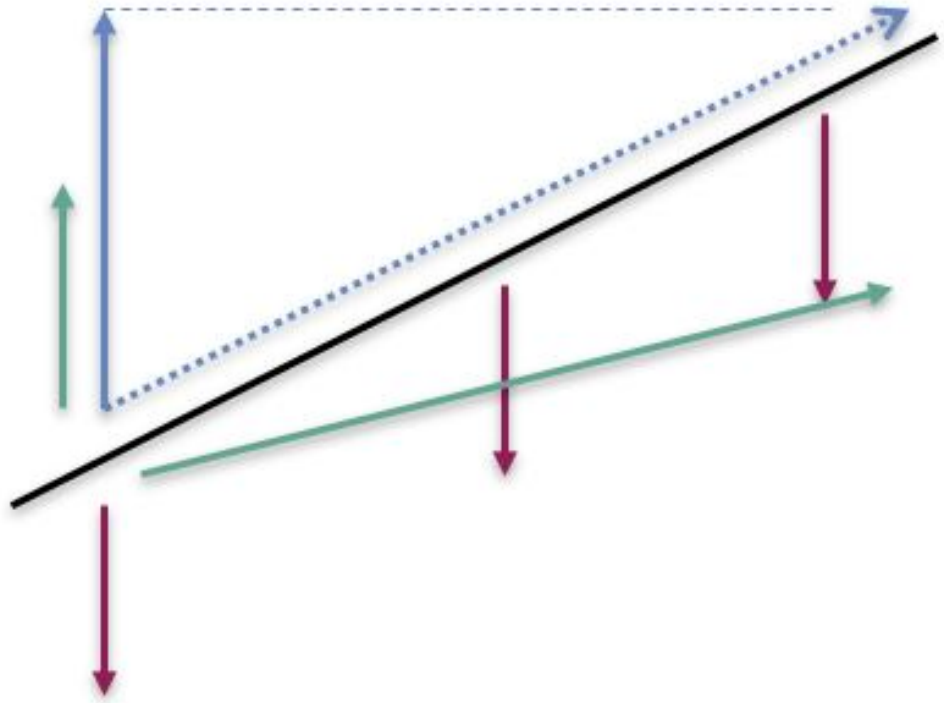

Figure 3.1: An illustration to clarify the conditions of unstable upgliding by an example described in subsection3.3.2. The black line represents an isentropic surface, on which an air parcel is advected by the blue dashed line (term two and three in equation 3.2), while the isentropic displacement is downward shown by the red arrows (first term in equation 3.2). Therefor the advection has to occur along the green line which trajectory has a slope less then the slope of the isentrope.

This directly implies that the value of $\left(\frac{\partial z_\theta}{\partial t}\right)$ should be half of the advection term for maximum efficiency. Therefore, efficiency should be described by a function which grows from zero if:

$$\left(\frac{dz}{dt}\right) \approx u\left(\frac{\partial z_\theta}{\partial x}\right) + v\left(\frac{\partial z_\theta}{\partial y}\right)$$

to a maximum (in absolute sense) if:

$$\left(\frac{dz}{dt}\right) = -\frac{1}{2}\left[u\left(\frac{\partial z_\theta}{\partial x}\right) + v\left(\frac{\partial z_\theta}{\partial y}\right)\right]$$

and back to zero if:

$$\left(\frac{dz}{dt}\right) \approx 0$$

When considering deviations from maximum efficiency, one can simply linearize the efficiency by considering only the first order term of the Taylor expansion. Obviously this approximation is valid in the small angle limit, which is typically satisfied for any isentropic surface encountered. This leads to the following result for the efficiency:

$$e \equiv \left|\frac{\frac{\partial z_\theta}{\partial t} + 0.5\,\mathbf{V}\cdot\nabla_h z_\theta}{0.5\,\mathbf{V}\cdot\nabla_h z_\theta}\right| - 1 \tag{3.5}$$

This equation makes use of the absolute height coordinate system instead of isobaric framework. This is important since pressure decreases logarithmic with height and thus, the analysis done in chapter 2 would otherwise not make sense. So in other words, the conditions for baroclinic energy conversion can be described in a absolute height coordinate system as well as a pressure coordinate system, however the efficiency can only be described in an absolute height framework. The maximum efficiency is not equal to 1, but to 0. Only in absolute sense the maximum efficiency is equal to 1. This does not matter for the rest of the analysis but is something to keep in mind.

3.3.4. Definition baroclinic energy conversion

This subsection is meant to summarize the findings of the previous two subsections. Subsection 3.3.2 describes the necessary conditions of baroclinic energy conversion while subsection 3.3.3 informed the reader on the definition of the efficiency term. This gives all the necessary information to quantify baroclinic energy conversion. When the conditions are met, vertical velocity gives an order to the amount of energy that can be converted. Small vertical velocities give rise to small changes in APE, following section 2.2. Furthermore, the efficiency determines to what extent vertical velocity is favourable for the conversion of energy. This can be summarized in the following definition of baroclinic energy conversion:

$$BEC \equiv Baroclinic\ energy\ conversion \equiv vertical\ velocity * efficiency \tag{3.6}$$

If and only if the conditions of equations 3.3 and 3.4 are fulfilled. Otherwise baroclinic energy conversion is zero. The vertical velocity in definitionn3.6 can be described by 'w' as well as 'ω'. In this study ω is chosen as vertical velocity and the units of BEC is therfore Pa/s.

4

Case study

Now that the definition of baroclinic energy conversion is settled and the method for studying this in the atmosphere is described it is time to test the theory to a real atmospheric example of Rossby wave breaking. This chapter is written to introduce the reader with the concerned case study of this thesis. This breaking event will be shown in a PV-θ perspective. Since potential vorticity has not yet been explained in this study, section 4.1 is written to inform the reader on the definition of potential vorticity. The consecutive section will show the breaking event in a chronological order. Also the cross section of the ridge of the wave will be shown. The combination of these two perspectives and accompanying explanation should give a clear view on the case study and Rossby waves in general. The last section will give remarks on diabetic effects in this case study.

4.1. Isentropic potential vorticity

Just like air parcels are bounded to isentropic surface because they conserve potential temperature under adiabatic circumstances, there is another atmospheric quantity for which is true which need extra explanation. This quantity is called ***Potential Vorticity*** (Π), and gives -as the name suggests- the potential for an air parcel to gain or loose vorticity. Absolute vorticity can be described as the addition of planetary- and relative vorticity. Planetary vorticity (f) is latitudinal dependent and describes the spin an air parcel has due to the spin of the earth, while relative vorticity (ζ) describes the vorticity relative to the earth. Isentropic density(σ) is inversely proportional to static stability, and describes the amount of mass between isentropic surfaces. Potential vorticity is defined as absolute vorticity divided by isentropic density, see equation 4.1.

$$\Pi \equiv \frac{f + \zeta}{\sigma} \tag{4.1}$$

4.1.1. Implications

The conservation of PV has large implications for atmospheric dynamics in general. The definition stated in subsection 4.1 hides some interesting facts about the relation between vorticity and static stability. The stratosphere is characterized by high values of PV due to the large vertical gradient of potential temperature, which by definition means a large static stability. Static stability is much lower in the troposphere, and a remarkable abrupt change of PV can be found where the troposphere morphs into the stratosphere. In fact, the definition of the stratosphere and troposphere can be solely described by its PV-value. The boundary between the troposphere and the stratosphere is called the tropopause. The dynamical tropopause is be defined as the 2 PV-unit surface.
Another striking result from subsection 4.1 is that the three terms of equation 4.1 are always in balance in adiabatic conditions. This has important consequences for the motion of the flow. For example when an air parcel with a certain PV is displaced meridionally, it finds itself in

a new environment with a different planetary vorticity. At this moment, the air parcel has to respond to this change in order to conserve its potential vorticity. However it can change its relative vorticity as well the isentropic density. A positive PV anomaly for example can be counteracted by increasing the relative vorticity and give the flow a (larger) cyclonic tendency. On the other hand, the static stability could be be increased to achieve the same result. How could one predict which process will occur? From the equation of PV inversion, Kleinschmidt found that **both** must occur Thorpe (1993). And that is exactly what can be observed in the atmosphere, as will be seen in the next section.

Section 4.1 was a small intermezzo on the definition of PV, necessary to understand next section and successive chapters. However, it only gives a very brief introduction and provides far from all the possibilities and implication of PV in atmospheric dynamics. More in-depth information can be found for example in (Hoskins' et al. (1985)). To this point is is important to understand the following three points:

- PV is conserved under adiabatic circumstances
- PV is a relation between the curl of the velocity field, planetary vorticity and static stability
- A change in planetary vorticity is counteracted by changes in relative vorticity **as well as** isentropic density

4.2. Rossby wave breaking in PV-θ perspective

Rossby wave breaking can be viewed in a potential vorticity-θ perspective. The 330K isentropic surface intersects the tropopause where the troposphere and stratosphere meet at this level. This is normally at latitudes with a large meridional temperature gradient, since the tropopause slopes downward in poleward direction, while the isentropic surface slopes upward. When PV is plotted on isentropic surfaces, there can be made a clear distinction between tropospheric air and stratospheric air. In this way Rossby waves can be visualized, areas which are occupied by troposphere air which 'normally' consists of stratospheric air show a wavy pattern. This also means that air which originally has low/high values of PV gets transported meridionally and therefore experiences an increased planetary vorticity. As described in subsection 4.1.1, potential vorticity is a conserved quantity. So a change in planetary vorticity has to be compensated by (anti-)cyclonic vorticity relative to the earth and an increase of isentropic density.

The following case study is a typical example of Rossby wave breaking. This subsection is written to show the process of wave breaking in the PV-θ perspective before continuing to the role of baroclinic energy conversion in this process.

Figure 4.1 shows the wave breaking event in a PV-θ perspective. The Rossby wave is overturns at approximately 12 March. At this moment, tropospheric air has penetrated as far north as 62°N. This can be seen by the large amount of 'blue' coloured air at these latitudes. The colour scheme represents potential vorticity, in which there is a change from blue to orange at 2 PVU. The solid black lines represent the Montgomery streamfunction. The Montgomery streamfunction is defined by equation 4.2 and is the isentropic analogy of geopotential. The streamlines from equation 4.2 are a representation for geostrophic flow and the gradient of Montgomery streamlines give an indication for the absolute wind velocity.

$$M = c_p T + g z \tag{4.2}$$

Tropospheric air that penetrated far north has experienced a large increase in planetary vorticity, so a response of the flow should be an increase in isentropic density and a decrease in relative vorticity to conserve potential vorticity. The anticyclonic tendency is noticeable when looking at the Montgomery streamlines in figure 4.1 in chronological order. The isentropic density however can not be seen from the top-view in figure 4.1, therefore a cross section is needed since isentropic density is inversely proportional to static stability. Figure 4.2 shows the longitudinal cross section of the same wave breaking event at 49°N, between 140°E

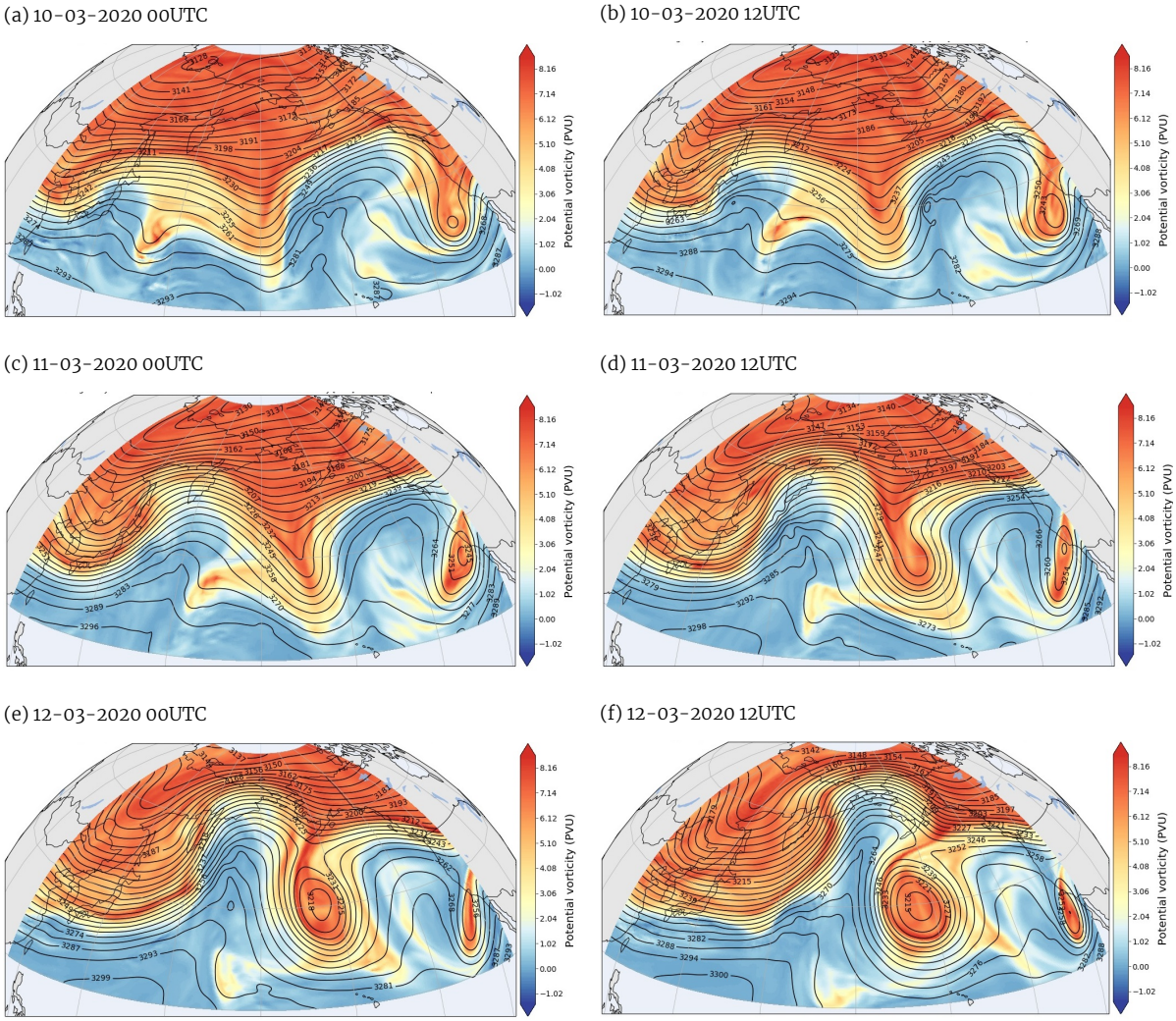

Figure 4.1: Multiple moments during the event of wave breaking visible at the 330K isentropic surface in which the colours represent PV [PVU]. Orange colours correspond to the stratosphere while blue colours correspond to tropospheric air masses. Black contour lines represent the Montgomery streamfunction.

and 195°E. The solid black lines and the colored highlighted lines show surfaces of constant potential temperature. The highlighted levels represent the levels of 300K, 315K, 330K and 350K which represent the different levels studied in this thesis. The colours in this figure represent again the potential vorticity. The dashed contours are contours of equal absolute wind velocity. It can clearly be seen that around the time the wave is captured by the cross section as shown in figure 4.2 the isentropes between 315K and 330K are diverging. This is exactly what is expected following the theory of subsection 4.1.1, The regions with the largest potential vorticity anomaly show an increase in isentropic density. Especially the 315K and 330K isentropes are divergent, implying the largest PV anomaly. The 330K isentropic surface follows approximately the tropopause and in the cross section this really looks like a ridge. Furthermore, it can be seen that the highest wind velocity can be found just under the tropopause, above the largest temperature gradients. This is no accident, but a response to the vertical integrated thermal wind balance. Furthermore, due to the divergence of isentropes in the upper troposphere, the isentropes in the lower troposphere are 'pushed' downward. This means that the lower troposphere has a positive temperature anomaly, and this is one of the characteristics of the ridge of a Rossby wave. At the same time the upper troposphere and lower stratosphere show a colder then normal tendency, which is noticeable by the raised isentropes. While this are all characteristics for an anticyclone, cyclones show opposite characteristics.

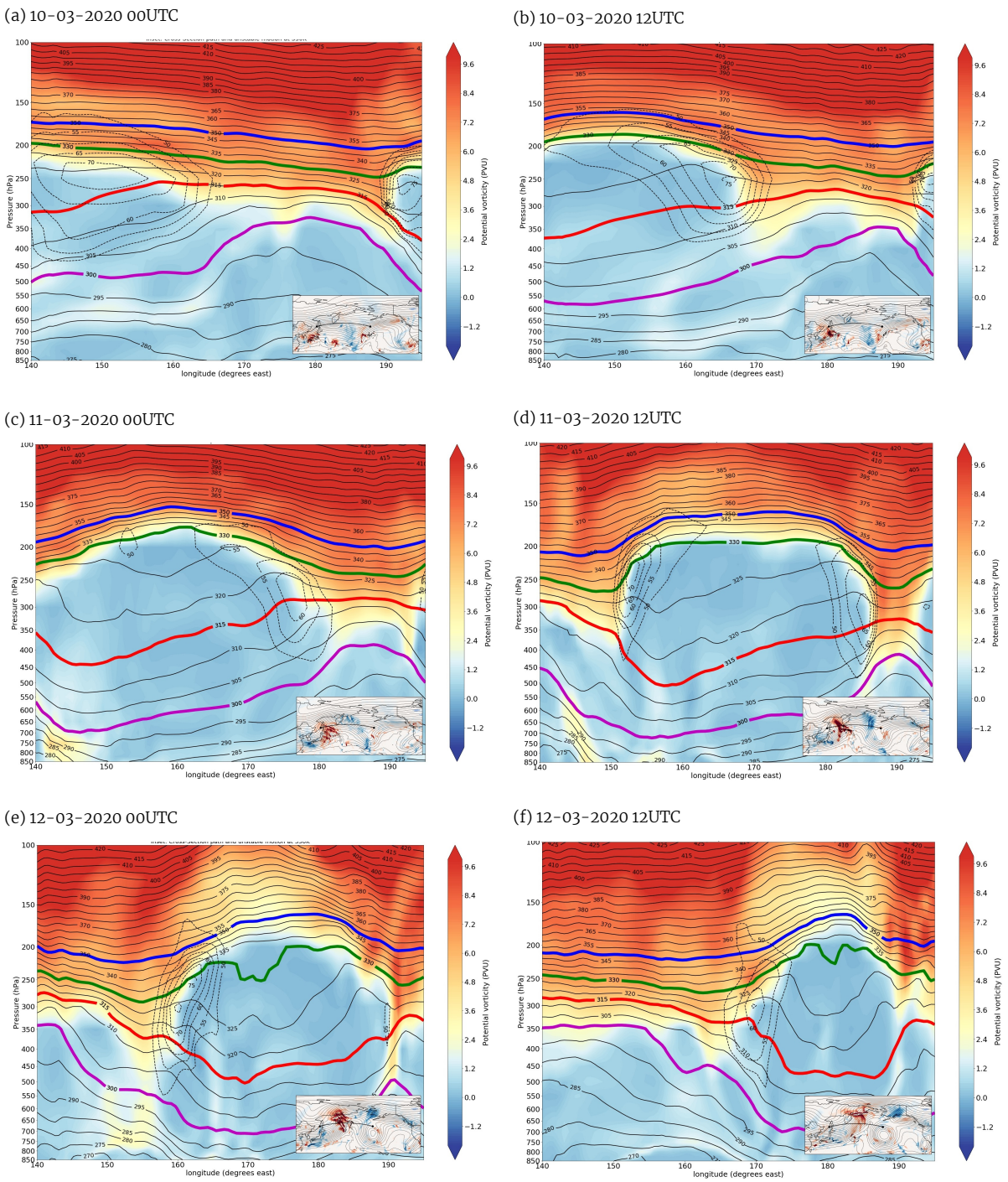

Figure 4.2: Longitudinal cross section at 49N, between 140E and 195E during multiple moments of a wave breaking event. Colours represent PV, black and highlighted solid lines represent surfaces of equal potential temperature and dashed contours represent absolute wind velocity. The inset figure illustrates where the cross section is taken.

4.3. Diabatic effects in the case study

During this study the main assumption is that large synoptic weather systems are adiabatic. However, relatively new research from Pfahl et al. (2015) suggests that this may be a bold assumption. This study suggests that latent heat release (diabatic effects) are of first importance for the formation and the maintenance of blocking events. It is stated that diabatic effects are of equal importance to blocking onset to the classical theory which describes the importance to the advection of low valued PV air from a tropospheric source. The study

(a) 11-03-2020 12UTC, 300K

(b) 11-03-2020 12UTC, 315K

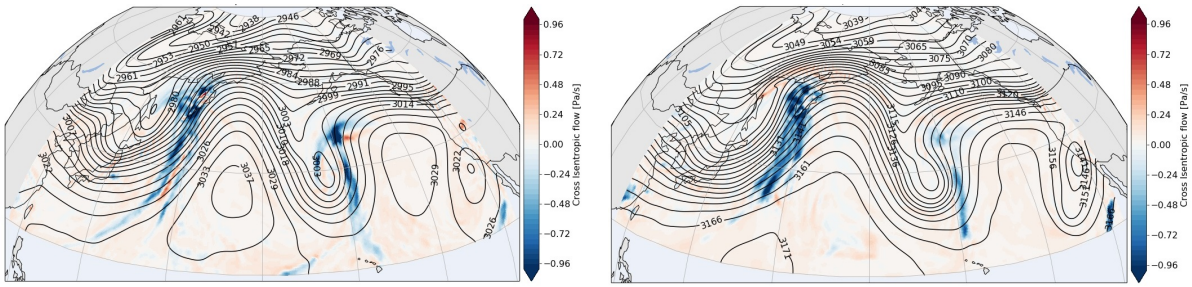

(c) 11-03-2020 12UTC, 330K

(d) 11-03-2020 12UTC, 350K

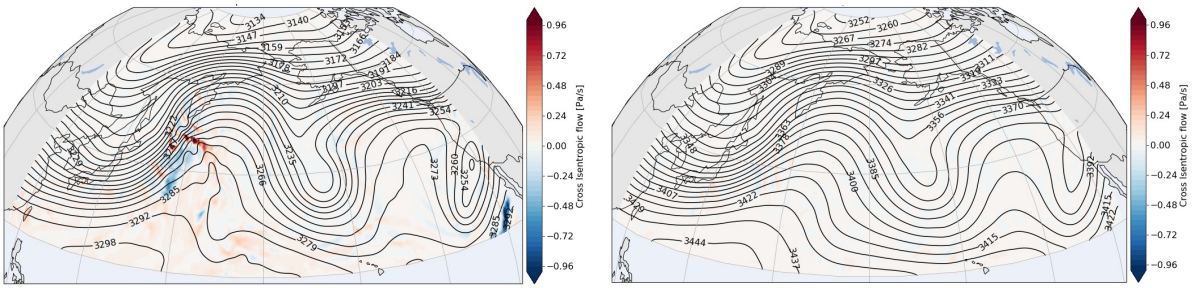

Figure 4.3: Visualization of cross isentropic flow, a measure of diabetic effects. Lower atmospheric levels show upward velocities due to latent heat release. Upper tropospheric and stratospheric levels are not or little directly influenced by this process.

found, via a Lagrangian model, that 30% to 45% or the followed air parcels which end up in the blocking anticyclone are heated by at least 2K. Latent heat release is responsible for creating PV at low levels and destroys PV at upper levels, meaning PV is lowered above level of maximum heating and increased below the this level. The authors state that for this reason latent heat release is of great importance for the onset of blocking anticyclones. They dedicate the mediocre prediction of blocking events to the ***'erroneous representation of latent heating in weather prediction models'***. Prominent researcher on this topic Woollings (Oxford University) recently confirms that latent heat release may play a more important role then expected until now. This gives enough reason to question the assumption of adiabatic conditions and study the effect of diabatic conditions on baroclinic energy conversion. Figure 4.3 shows regions where diabatic effects may play an important role at one moment during the growth of the wave at the four different isentropic levels. The coloured regions are regions of cross isentropic flow. Cross isentropic flow is only possible when air parcel experience some sort of diabatic heating or cooling, since in adiabatic conditions air parcels are bounded to isentropic surfaces by definition. These regions give therefore a good representation of diabatic effects. The intensity of the coloured areas represent the cross isentropic vertical velocity. However, the lack of upward cross isentropic motion reveals that diabatic cooling is far less pronounced on the chosen levels in comparison with diabatic heating due to condensation of water vapour. Velocities as large as -1 Pa/s are found upstream of the ridge and downstream of the trough. This indicates a warm conveyor belt which is responsible for the poleward transport for large amounts of mass, heat and moisture. Due to the upward motion air parcels experience when moving in a northward direction huge amount of latent heat releases in the form of cloud formation. However this is to a large extent height dependent, specific isentropic levels are located far above the levels of condensation and are not really affected by this process. This can be seen in figure 4.3 where a comparison of cross isentropic flow between different levels is made. 300K and 315K levels are obviously subjected to latent heat release, while the levels 330K and 350K are not (or less) affected by diabatic effects. Consequences of latent heat release on baroclinic energy conversion will be discussed in the next chapter.

5

Results and discussion

To the authors knowledge there is no research available on quantifying baroclinic energy conversion as done in this study, where an efficiency term is calculated explicitly. However, the idea that potential energy can be seen as a source for energy in meteorology was already described by in 1905 by the German meteorologist Margules. The term of available potential energy was formally described by Lorenz in 1955, within his work on the general circulation (Lorenz, 1955). Van Delden (1999) argued that isentropic slopes are a measure for baroclinic development. Isentropic slopes are later used in the work of Papritz and Schemm (2013) in which it was found that growing baroclinic cyclones are reflected by adiabatic flattening of isentropes. The authors also found that climatologically this tendency is balanced by the generation of slope due to diabatic effects. The study of van Delden and Neggers (2003) uses the isentropic slope for the analysis of cyclogenesis at upper levels. The authors use the definition of energy conversion as described by Green (1979) for their analysis and reasoned that large areas of ***'unstable (isentropic) downgliding'*** are actually necessary to realise a tropopause cyclone. For this, the authors make use of the ERA-interim dataset for designating areas where APE can be converted into KE. However, due to relative low temporal and spatial resolution of the ERA-interim dataset the results are presented with the necessary caution.
This study continues on work from van Delden and Neggers (2003), but makes use of the recently released ERA-5 reanalysis, which enables calculation of temporal and spatial derivatives with unprecedented accuracy. This also introduces the possibility to quantify baroclinic energy conversion with the use of the efficiency term as presented in section 3.3.3. This chapter is meant to present and discuss the results of baroclinic energy conversion, elucidate the underlying processes, and map its consequences for Rossby wave breaking. First a complete overview will be given on the behaviour and details of BEC on two different levels, the 315K isentropic surface and the 330K isentropic surface. These two levels are interesting as the 330K level represents the upper troposphere at which the diabatic effects are negligible and the highest wind velocities can be found. In section 4.3 is was shown that diabatic heating by the process of condensation plays a large role in the warm conveyor belt at lower levels, therefore processes on the 315K surface are not under complete adiabatic conditions. Since the methodology form chapter 3 is completely based on the assumption that synoptic weather events are close to adiabatic conditions the 315K surface is an interesting level to look at. Some remarks will be made about the 300K and 350K surfaces, however these levels will not be analysed in great detail because they show a lot of similarities compared to the two levels which are fully analysed. Secondly, the implications of BEC on the jetstreak formation or strengthening will be analyzed. In an Eulerian framework as well as a Lagrangian framework the velocity field will be related to the regions of unstable up/downgliding. The influence of the velocity field on Rossby amplification and breaking is described in detail in section 5.4, which also discusses the consequences of baroclinic energy conversion for the the secondary circulation. The last section will be concerned with the adiabatic assumption and especially with recently made claims concerning diabatic effects on blocking onset (Pfahl et al. (2015)).

5.1. Baroclinic energy conversion on the 330K surface

(a) 10-03-2020, 00UTC

(b) 10-03-2020, 12UTC

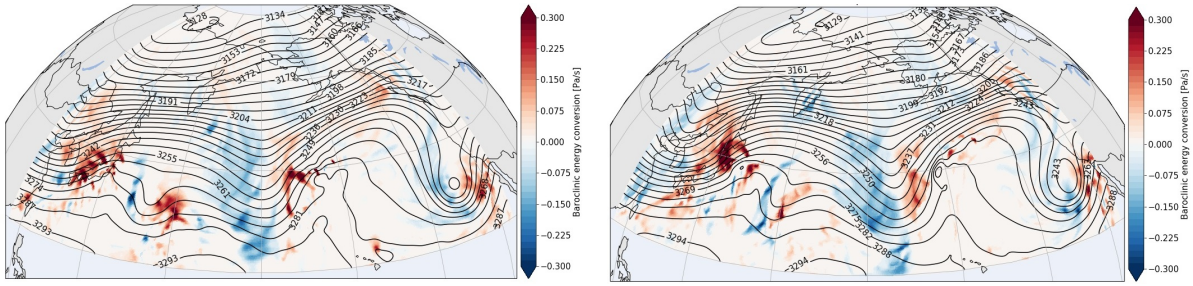

(c) 11-03-2020, 00UTC

(d) 11-03-2020, 12UTC

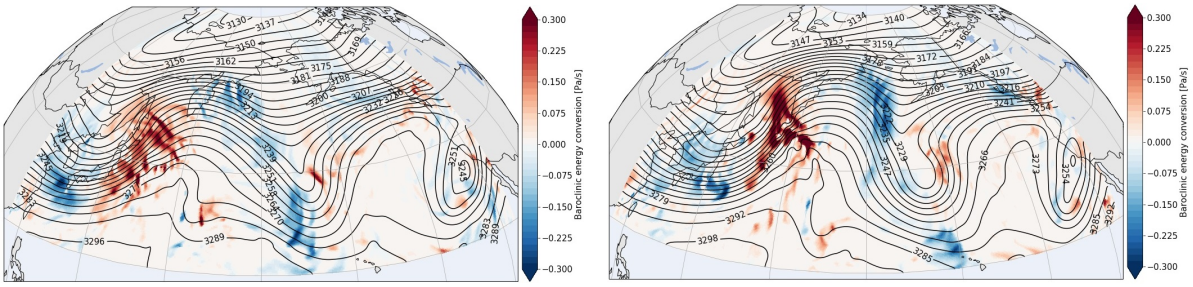

(e) 12-03-2020, 00UTC

(f) 12-03-2020, 12UTC

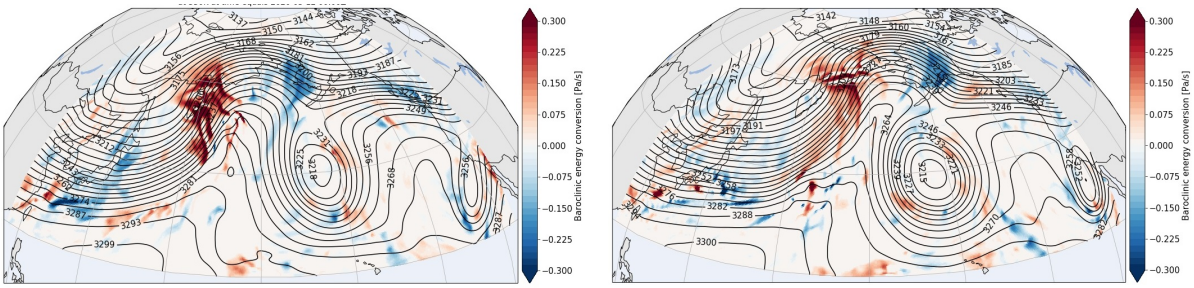

Figure 5.1: Development of baroclinic energy conversion during a growing Rossby wave. Red colours represent BEC via unstable upgliding, while blue colours represent BEC via unstable downgliding. The most intense areas of BEC can be found at the meridional moving part of the Rossby wave in the vicinity of relative vorticity minima and maxima.

This subsection is written to make remarks about the movement of regions where baroclinic energy conversion is possible. Figure 5.1 shows the different stages during Rossby wave propagation and the associated intensity of BEC on the 330K level. The black solid lines represent the 'Montgomery streamfunction', the filled contours represent areas of unstable up- and downgliding, blue colors correspond to unstable downgliding, while red colors represent unstable upgliding. The intensity of the colours represents the intensity of baroclinic energy conversion, as stated in chapter 2 this means adiabatic vertical velocity multiplied with efficiency. Intense regions of baroclinic energy conversion are noticeable along the meridional gradient of the Rossby wave, especially in the vicinity of relative vorticity maxima and minima. This already suggests that this mechanism could play a role in Rossby wave amplification and thus accelerating the jetstream. Another distinctive property of these regions is that they all seem to move, not one region can be pointed out that is stationary relative to the earths surface. This supports the proposed theory on baroclinic energy conversion. As discussed in chapter 2.2, regions of unstable up- and downgliding use the gradient of the isentropes to lower the potential energy of the atmosphere in favour of kinetic energy. Since the gradient of the isentropes is used as an energy supplier, this process must be accompanied by flattening of the isentropes. The consequence is that the potential for baroclinic energy conversion must be locally lowered at the rear end of these areas, while at the front of these areas

(a) 10-03-2020, 00UTC

(b) 10-03-2020, 12UTC

(c) 11-03-2020, 00UTC

(d) 11-03-2020, 12UTC

(e) 12-03-2020, 00UTC

(f) 12-03-2020, 12UTC

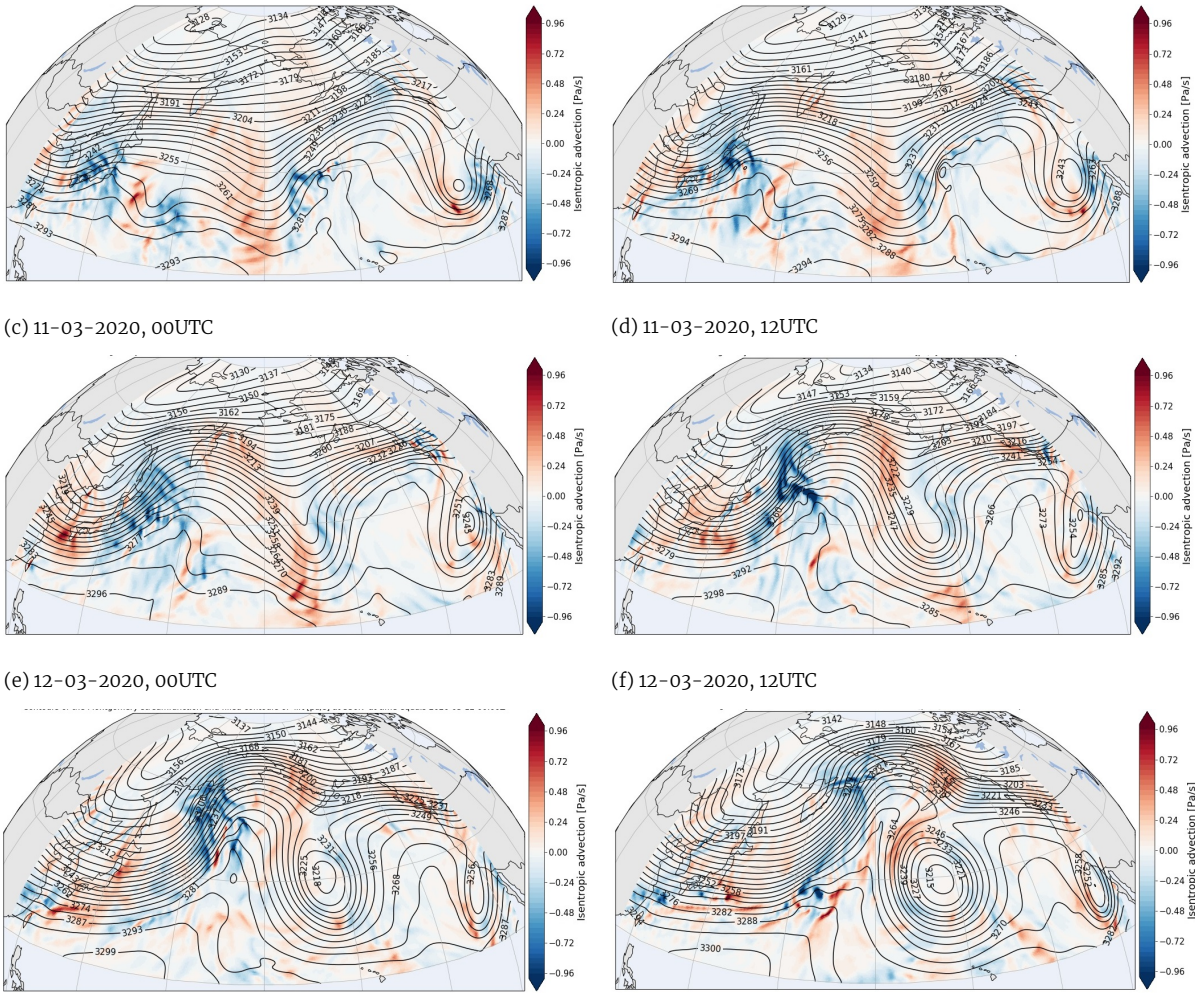

Figure 5.2: Development of the vertical velocity due to the gradient of the isentropic surfaces. The regions with (absolute) large vertical velocities are constantly moving and highly related to the regions of intense BEC.

the gradient of the isentropic surfaces increases and thus also the potential for baroclinic energy conversion. Furthermore this implies that when the mechanism of BEC is initiated, it is (for a part at least) self maintaining, and thus, the wave has to move because of the constant changing environment of the isentropic surfaces, which can be seen in figure 5.1.

If isentropic flattening is indeed caused by baroclinic energy conversion this should leave an additional signature in the vertical velocity profile. Vertical velocity (in absolute sense) should decrease at the rear end of regions of BEC and should increase in the vicinity of the epicentre of BEC areas. This is shown in figure 5.2, where it can be clearly seen that the regions of large absolute vertical velocities due to advection along sloped isentropes coincide with the regions of intense BEC.

Another interesting quantity to look at is the ‘efficiency’ term of BEC which is independent of absolute vertical velocity and maps all the regions where BEC is possible. Obviously the regions with the highest (in absolute sense) efficiency should correspond with the most intense regions of BEC. Figure 5.3 maps the efficiency for one moment during the wave growth and it can thus be concluded that in large parts of the atmosphere air parcels move with a slope smaller than the slope of the isentropes. This emphasizes the presence of baroclinicity in the mid-latitudes, and the extreme large areas indicate that the atmosphere always tries to be in a state of minimal potential energy which leads to a very dynamical behaviour. This would be in line with model experiments from O’Gorman and Schneider (2008), in which the authors found that changes in kinetic energy approximately scale linear with the available potential

energy averaged over the baroclinic zone. The areas where BEC has a high (in absolute sense) efficiency correspond to the regions of intense BEC from figure 5.1. However, not in all regions of high efficiency (in absolute sense) does a significant amount of BEC occur, emphasizing the importance of vertical velocity in the process of BEC. The fact that not all these regions can be seen back in the mapping of BEC could only be described by the lack of vertical velocity.

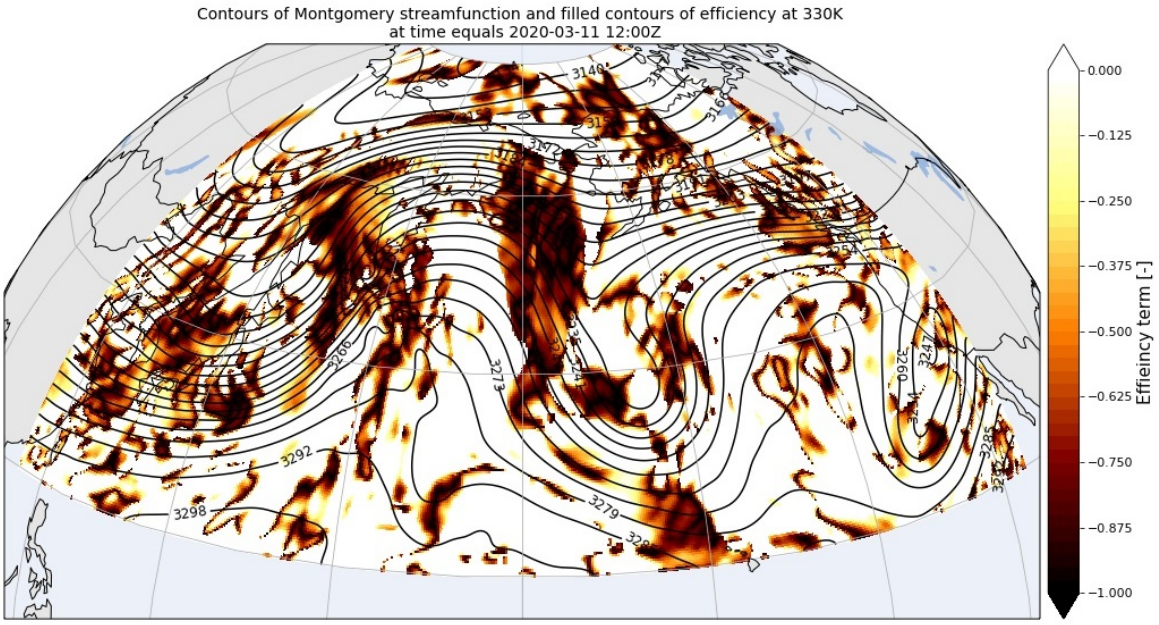

Figure 5.3: Regions which fulfill the conditions for baroclinic energy conversion get an efficiency assigned which is visualized in this figure for 11-03-2020, 12UTC. The efficiency term has a maximum magnitude of one and a minimum magnitude of zero. Grey regions do not fulfill the criteria for BEC hence do not have an efficiency value

5.2. Baroclinic energy conversion on the 315K surface and influences of diabetic effects

The 315K surface is interesting to look because, as opposed to the 330K surface, diabatic effects play a (much larger) role, which was also already stated in section 4.3. As stated in subsection 3.3.2, the fourth term of equation 3.1 was neglected, which is a good approximation for upper levels where the influence of diabatic effects is negligible. Diabatic effects could however potentially bring an additional contribution to the motion relative to the isentropes. This section is written to analyse and explain the details of diabatic effects on BEC. The reasoning that areas of BEC have to move forward due to the tilting of isentropes still stands, however the three dimensional pattern gets more complicated due to the influence of diabatic effects.

To study the influence of diabatic effects, one moment during the growing wave is taken and the individual terms from equation 3.2 are plotted. For comparison, this is done for the 315K level as well as the 330K level which are shown in figures 5.4 and 5.5 respectively. In the top two subfigures (figures 5.4a and 5.5a) the colourscheme represent BEC. In the middle subfigures (figures 5.4b and 5.5b) the colourscheme represents the vertical velocity of air parcels due to advection along sloped isentropes, which is the second and third term from equation 3.2 combined. Figures 5.4c and 5.5c show the vertical velocity due to the displacement of isentropic surfaces, which is the first term in equation 3.1. The blue contours in all the subfigures represent the cross isentropic flow for absolute values greater than 0.2 Pa/s. Dashed contours represent negative values. It can be clearly seen that there is an area of quite intense upward isentropic vertical displacement at 315K to the west of the area of latent heat release (figure 5.4c) which is not noticeable at 330K (figure 5.5c). This can be explained by two mechanisms. Firstly, one of the characteristics of the interior of the ridge are higher temperatures than normal in the lower troposphere (see figure 4.2 in section 4.2) this means

(a) 11-03-2020 12UTC, baroclinic energy conversion, 315K

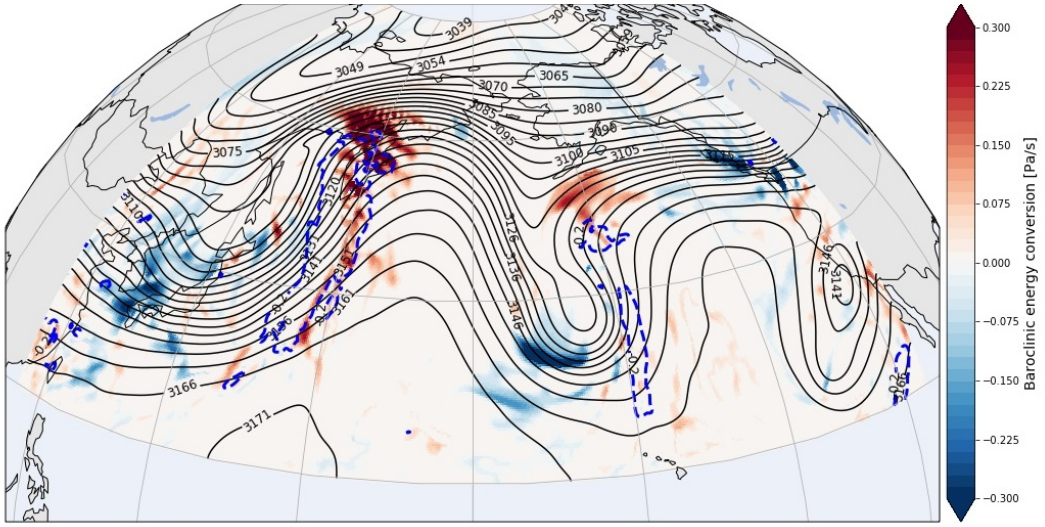

(b) 11-03-2020 12UTC, isentropic advection, 315K

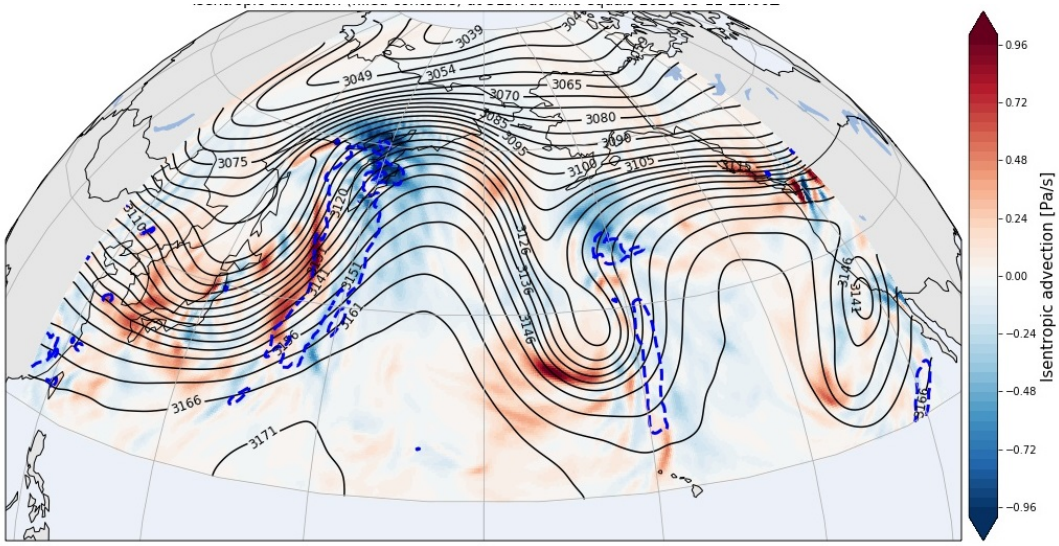

(c) 11-03-2020 12UTC, isentropic displacement, 315K

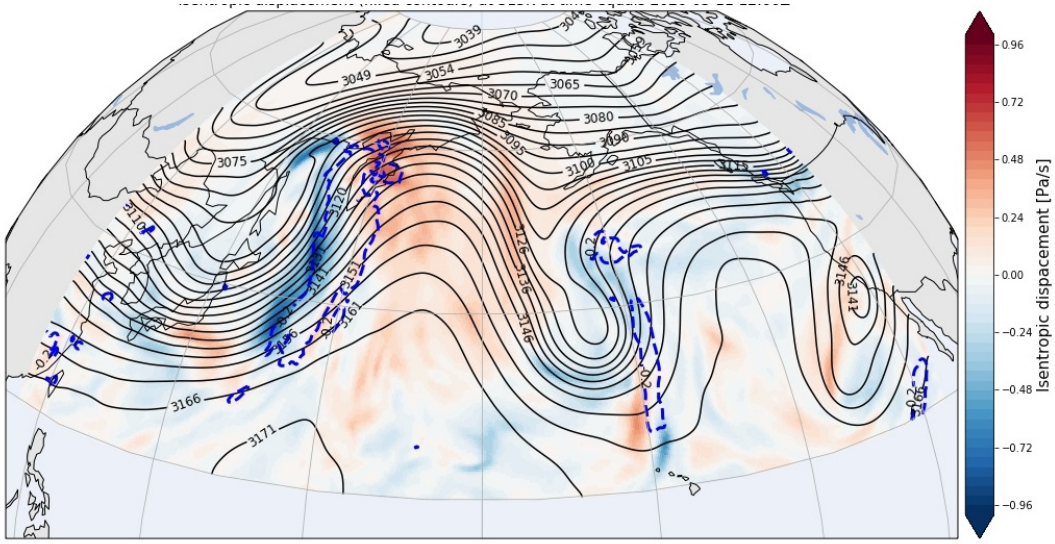

Figure 5.4: Different processes from equation 3.2 showed at the 315K level. (a) shows baroclinic energy conversion and cross isentropic flow for 11-03-2020, 12UTC, while (b) shows vertical velocity due to advection along isentropes instead of BEC. (c) on its turn shows vertical displacements of the isentropes

(a) 11-03-2020 12UTC, baroclinic energy conversion, 330K

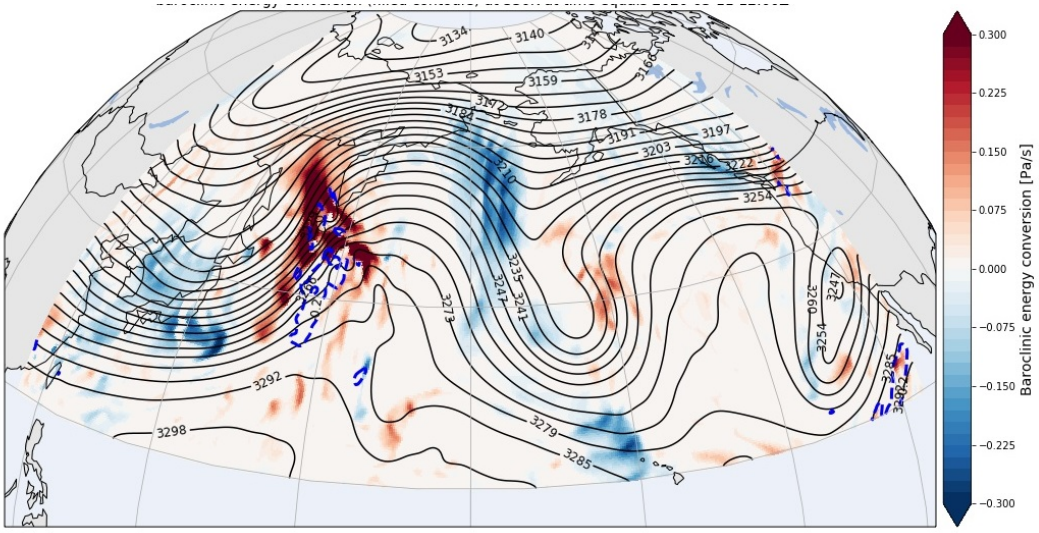

(b) 11-03-2020 12UTC, isentropic advection, 330K

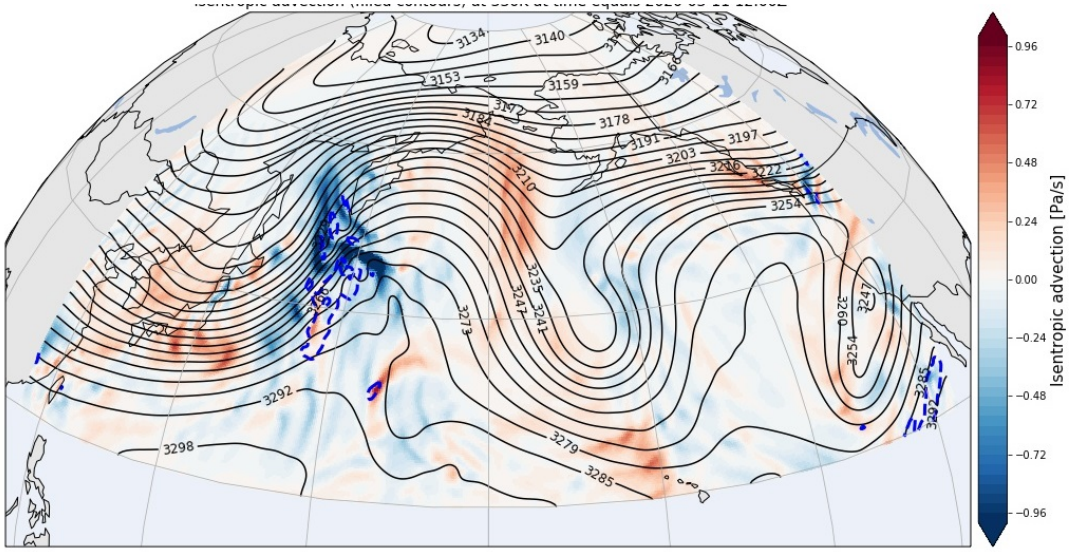

(c) 11-03-2020 12UTC, isentropic displacement, 330K

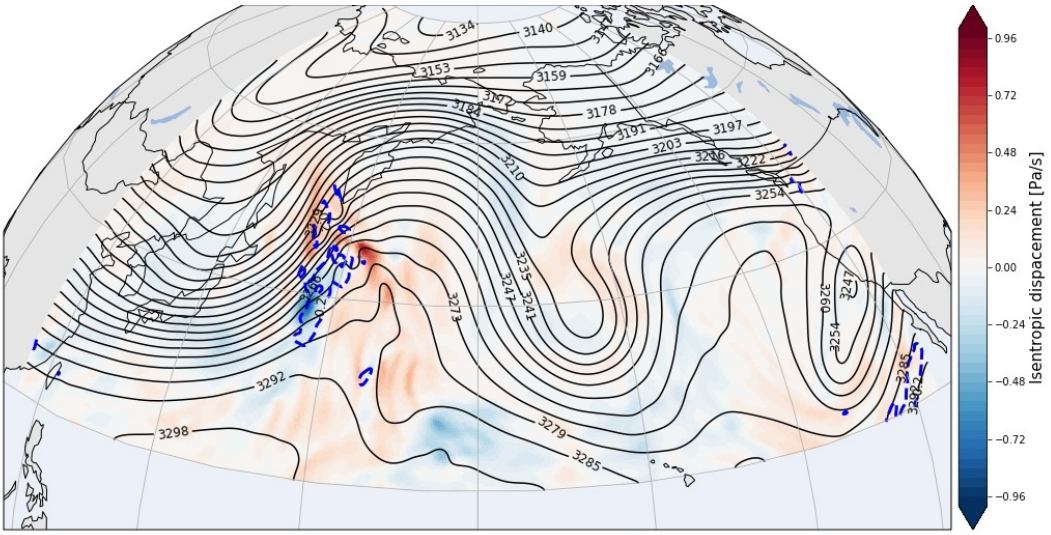

Figure 5.5: Different processes from equation 3.2 showed at the 330K level. (a) shows baroclinic energy conversion and cross isentropic flow for 11-03-2020, 12UTC, while (b) shows vertical velocity due to advection along isentropes instead of BEC. (c) on its turn shows vertical displacements of the isentropes

that the isentropes of the lower troposphere in the interior of the ridge must descend as the PV anomaly at upper-levels become more negative. This can be clearly seen in figure 5.4c, where large red areas are visible in the interior of the ridge, meaning that the isentropic level is descending. On the other hand, at the 330K level (figure 5.5c) this process is less dominant, and sometimes the isentropic level even ascends, while the 315K isentropic surface descents. At that time, the isentropic density increases, indicating a negative PV anomaly. This has the consequence that locally, on the edge of the PV anomaly the isentropes have to tilt, hence the upward coming 315K isentrope on the poleward side of the growing wave.

Secondly, latent heat release has the same effect as the PV anomaly. Below the regions of maximum heating, isentropes bulge downward, and the cross isentropic flow at 315K and the (almost complete) absence of it at 330K hints that maximum heating is above or around this level. Therefore, it may come as no surprise that to the west of the boundary of latent heat release, the isentropic surfaces bulge upward due to the tilting effect. In contrast, at the east side boundary of latent heat release this process is not very distinctive and this may be due to the dominant effect of the PV anomaly. The fact that the isentropic vertical displacement is distinctively upward west of the area of latent heat release (see figure 5.4c), means that unstable upgliding is impossible, and this explains the lack of BEC at the 315K surface (figure 5.4a), in comparison to the 330K surface (figure 5.5a).

Furthermore, the regions that are pointed out to be favourable for BEC at 315K still need some kind of verification. The consequence of diabetic effects is predominantly upward cross isentropic flow due to latent heat release in the warm conveyor belt. This means that particular regions of unstable upgliding could potentially show incorrect results, when regions of cross isentropic flow and baroclinic energy conversion overlap. As discussed, diabatic effects (term four in equation 3.1) bring an extra term for motion relative to the slope of the isentropes.

Figures 5.4a shows on 315K the contours of cross isentropic flow with a vertical velocity of -0.2 Pa/s (dashed, blue) and BEC by coloured shadings. Motion that, in adiabatic conditions has a slope smaller than the slope of the isentropes could potentially not fulfill this requirement due to the contribution of diabetic vertical velocity (term four in equation 3.1). Although it seems that the regions of baroclinic energy conversion are somewhat leading in front of the regions of cross isentropic flow, this is not always the case. Especially in the vicinity of relative vorticity maxima/minima diabatic effects may jeopardize the results, meaning that some BEC regions may be wrongly designated as such.

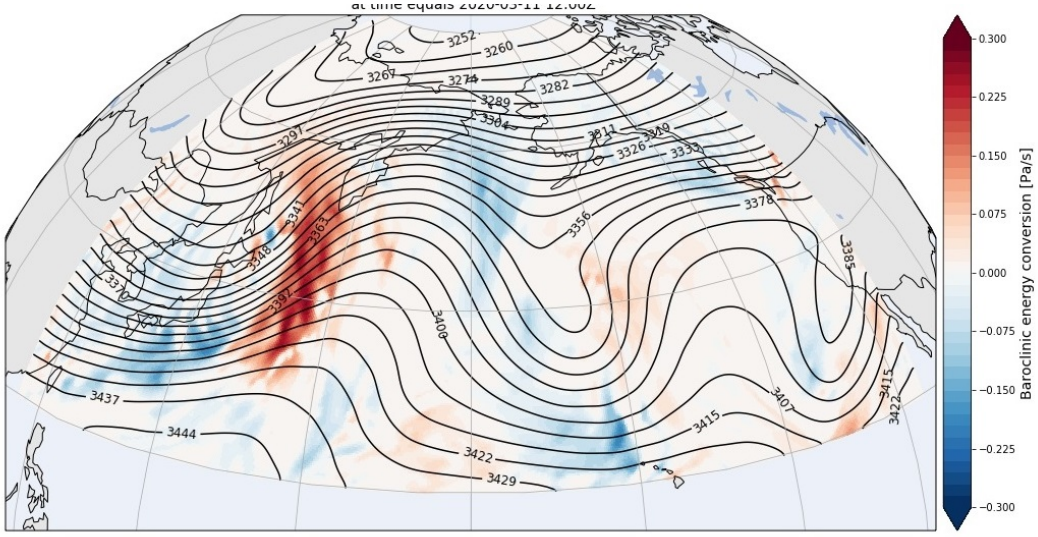

Figure 5.6: Baroclinic energy conversion at 350K at 11-03-2020, 12UTC.

5.3. The 300K and 350K surface

The 300K and 350K surface are also analysed, however, the 300K surface shows a lot of similarities with the 315K surface and is therefore not presented as it does not provide any additional insights. The 350K surface stands out, since this level lies predominantly in the stratosphere and not in the troposphere. Isentropic surfaces in the stratosphere are far less subjected to large temperature gradients compared with those in the troposphere. Therefore vertical velocities are smaller, yet still distinctive areas of BEC can be seen. It shows a lot of similarities with the 330K isentrope, the difference is that at 350K the intensity of BEC is less variable and more spread out. That can be seen when figure 5.6 is compared with subfigure d from figure 5.1.

5.4. Implications for Rossby wave amplification

The previous sections have emphasized that a large part of the atmosphere in the mid-latitudes is potentially suitable for the mechanism of BEC, and that the intensity of this process is mainly described by the vertical velocity. Especially at the level were the jetstream lies, approximately at 330K, there is an intense BEC region upstream of the wave prior to reaching the relative vorticity minimum. The following section will be dedicated to jetstreak formation by BEC and the link to Rossby wave breaking. The next subsection will show results of baroclinic energy conversion in relation with absolute wind velocity. The expectation is that jetstreaks overlap with regions of BEC. The successive subsection is dedicated to the path of individual air parcels. A moving frame of reference tracks different air parcels and the expectation is that these air parcels experience accelerations when entering intense regions of BEC. If this is true and accelerations arise, geostrophic balance will be no longer sufficient to describe the flow. The third subsection will explain how deviations from geostrophic balance react to the acceleration of the flow, and which role the secondary ageostrophic circulation has in Rossby wave amplification.

5.4.1. Jetstreak formation/strengthening

The jetstream is the consequence of the vertical integrated thermal wind. The boundary where the temperature gradient is reversing is also the level where wind velocities are strongest. This band of strong wind is called the jetstream and lies just underneath the stratosphere, around the 330K isentropic surface. At this level the vertical integrated thermal wind is maximum and changes in kinetic energy are more probable to be attributed to BEC in comparison with lower levels. It is for this reason that this level will be analysed to study the relation of kinetic energy and BEC. Furthermore, as was discussed earlier, diabatic heating may influence the results of BEC on the 300K and 315K isentropic surfaces, another reason that these levels are less suitable for a reliable analysis.

Figure 5.7 shows the absolute wind velocity (measure of kinetic energy) in black contours, while the the colours represent the intensity of BEC, during different stages of Rossby wave propagation. This figure strongly suggests a correlation between the gain in kinetic energy and regions where potential energy is lost. It is striking that the largest wind speeds are overlaying regions of BEC, especially during later stages of wave growth. This implies that this process is, at least partly, responsible for steering the jetstream by giving it an extra meridional impulse, causing the Rossby wave to grow. This suggests that the Rossby wave grows due to BEC. The mechanism of BEC could therefore be a good proxy for baroclinicty in the mid-latitudes and therefore an important indicator in the potential for Rossby waves to grow and eventually break. A jetstream which grows further north than usual also advects more air with low PV values into the ridge which in turn, due to the large gain in planetary vorticity, has to respond by strong anticyclonic tendencies and large isentropic densities there where the PV anomaly is largest.

(a) 10-03-2020, 00UTC, 330K

(b) 10-03-2020, 12UTC, 330K

(c) 11-03-2020, 00UTC, 330K

(d) 11-03-2020, 12UTC, 330K

(e) 12-03-2020, 00UTC, 330K

(f) 12-03-2020, 12UTC, 330K

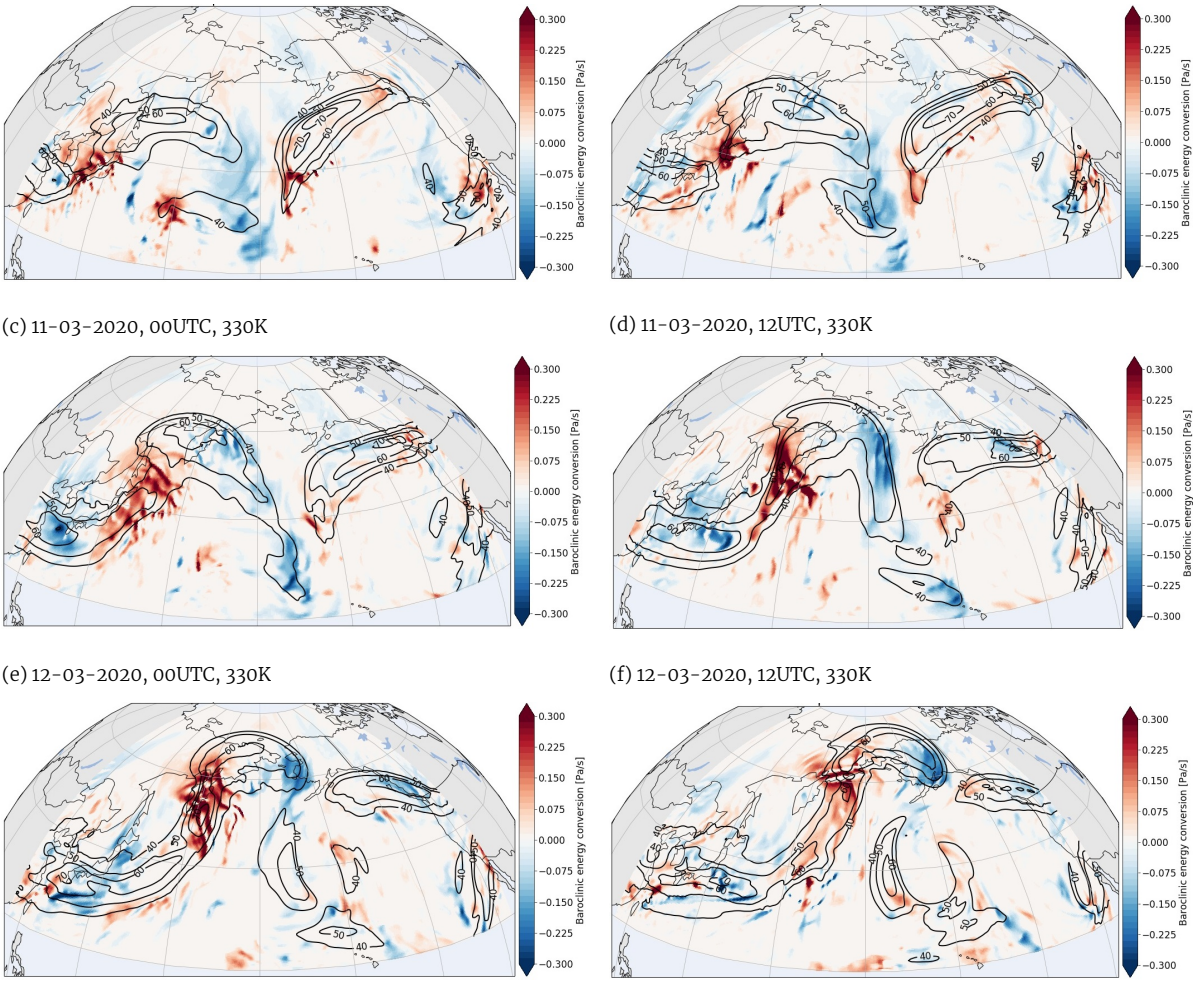

Figure 5.7: Baroclinic energy conversion (colours) and contours of absolute wind velocity (contours) at 330K at different moments during the event of wave breaking

5.5. Lagrangian model

Gains in kinetic energy also imply that individual air parcels experience an acceleration in the vicinity of regions of BEC. Twenty air parcels are released in a small area on the 330K isentropic level and followed using a moving frame of reference. The ERA-5 reanalysis dataset has a temporal resolution of one hour and a spatial resolution of fifteen arcminutes. The temporal resolution is increased to a quarter of an hour by linear interpolation. Hence every quarter of an hour the position of each individual air parcel is estimated, after which linear interpolation between the four surrounding data points is used for calculating quantities such as the magnitude of the absolute wind velocity or BEC.

The twenty air parcels are followed for the duration of 13 hours. Given that there is a datapoint every fourth of an hour means that the total number of datapoints is 1280. The path of the air parcels is shown in figure 5.8. The expectation is that individual air parcels will experience an acceleration when moving through the most intense regions of BEC.

5.5.1. Absolute windspeed

In order to study the relation between kinetic energy and BEC, a scatterplot is made with BEC on the y-axis and absolute wind velocity on the x-axis. The results are shown in figure 5.9 and every colour, which corresponds with the colour in figure 5.8, represents an air parcel.

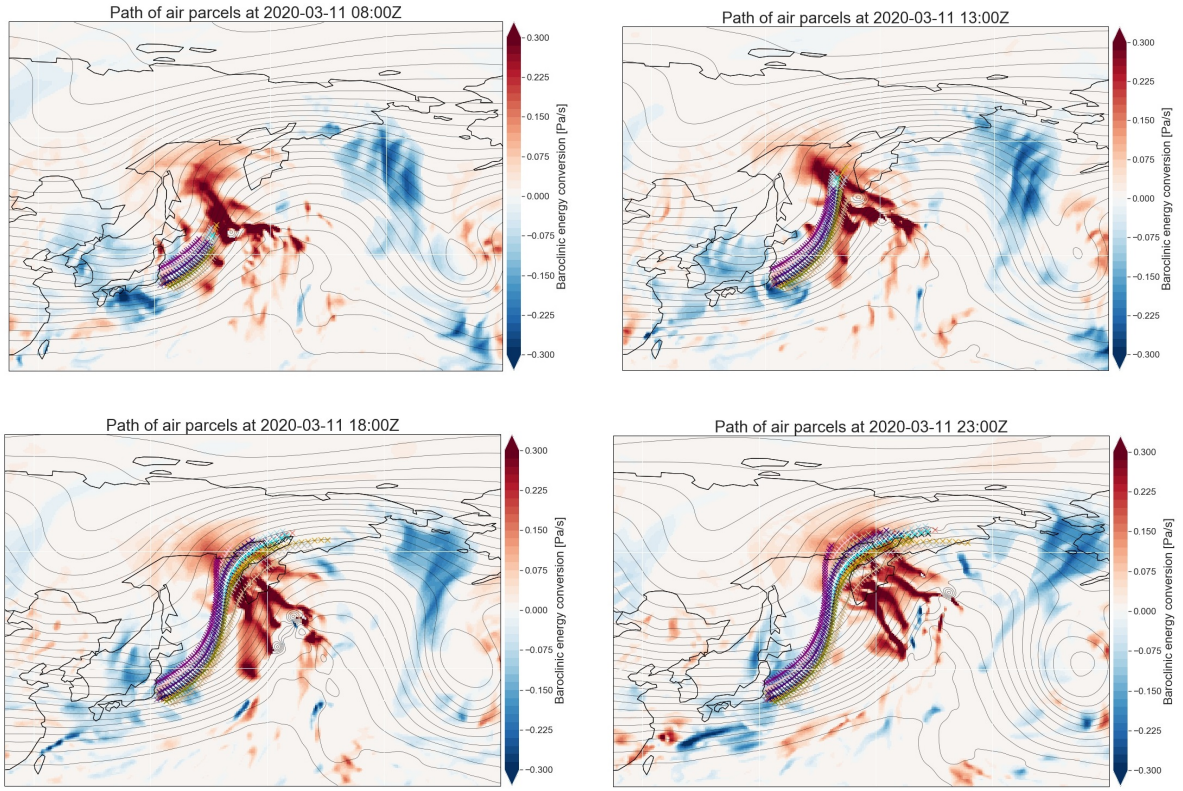

Figure 5.8: Path of 20 air parcels followed with a moving frame of reference

The variability is higher than expected and therefore it is hard to draw decisive conclusions regarding the exact relation between BEC and absolute wind velocity. However, a few interesting remarks regarding the pattern can be made. It can clearly be seen that high wind velocities are no certainty for large values of BEC. This comes as no surprise since the jetstream is dependent on more factors then only the intensity of energy conversion. Moreover, the main driver for the jetstream is the vertical integrated thermal wind(Woollings et al. (2010)). On the other hand, intense regions of BEC seem to be a certainty for large wind velocities. The data points all fall in a approximated right triangle, with the right angle in the lower right corner. It is striking that there are no data points in the top left corner, suggesting that relative weak wind velocities are never associated with intense baroclinic energy conversion. This means that intense baroclinic energy conversion is correlated with high wind velocities, while high wind velocities are no certainty for intense BEC.

5.5.2. Acceleration

Another interesting quantity to look at is the acceleration of the air parcels, because the formation or strengthening of jetstreaks has to be accompanied by accelerations of the jetstream. It is therefore expected that intense regions of BEC are related to accelerations of the flow. Figure 5.10 shows the scatterplot with accelerations on the x-axis and BEC on the y-axis. In total, 518 datapoints experience a negative acceleration while 762 datapoints experience a positive acceleration. The pattern is again characterized by a large variability, making it hard to draw decisive conclusions. It seems however that the mean value of BEC is higher for air parcels that experience a positive acceleration. The mean, median, and standard deviation of BEC for air parcels that experience positive and negative accelerations respectively are summarized in table 5.1. It comes at no surprise that the mean and median value of BEC are approximately twice as large for air parcels that experience a positive acceleration in comparison with air parcels that experience a negative acceleration. But again, conclusions are hard to draw since the difference of mean values of BEC are less than the standard deviation.

Figure 5.9: Scatterplot with BEC on the y-axis and absolute wind velocity on the x-axis, in which the datapoints correspond to the 20 followed airparcels.

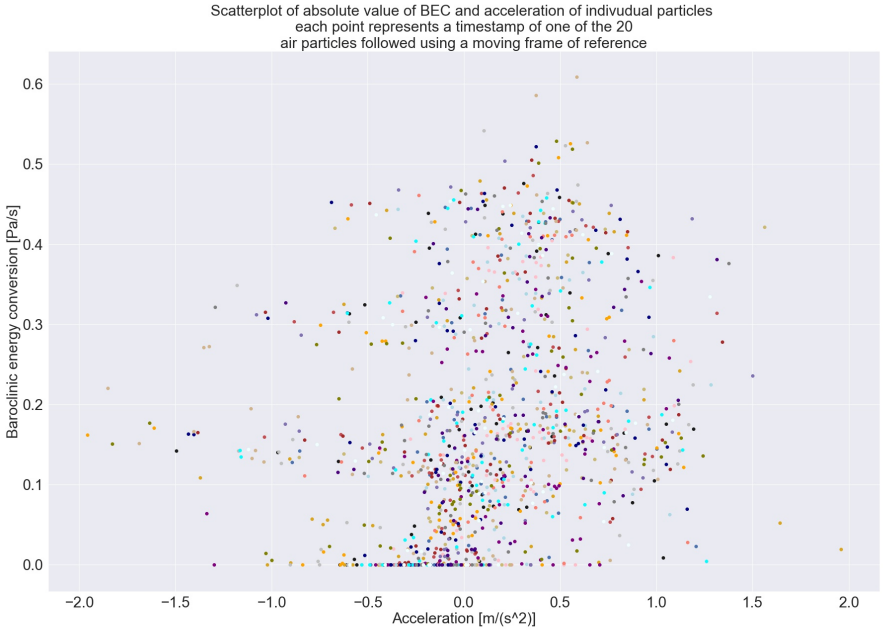

Figure 5.10: Scatterplot with BEC on the y-axis and air parcel accelerations on the x-axis, in which the datapoints correspond to the 20 followed airparcels.

Table 5.1: Summarizing table for the mean value, the median and the standard deviation of BEC for air parcels that experience a positive and negative acceleration respectively

–	*Positive acceleration*	*Negative acceleration*
# Data points	762	518
Mean value BEC [Pa/s]	0.217	0.117
Median value BEC [Pa/s]	0.178	0.093
Standard deviation BEC [Pa/s]	0.141	0.121

5.5.3. Summary

In the Eulerian frame it was striking that regions of BEC are overlapping with regions of large wind velocities. However, from the analysis in a Lagrangian frame it is difficult to substantiate these claims with hard evidence, although all arrows point in the direction of the mechanism of BEC being indeed (partly) responsible for the formation or strengthening of jetstreaks. Further research could focus on doing more elaborated experiments in order to find more substantiated relations between jetstreaks and BEC.

5.6. Ageostrophic wind

Accelerations of the main flow are per definition impossible in geostrophic balance, therefore an ageostrophic circulation has to occur due to observed accelerations. This section will give the ageostrophic wind due to accelerations on two levels, and explain their differences.

Figure 5.11 shows the Montgomery streamfunction (grey contours) as well as absolute windspeed (colourscheme) and ageostrophic motion (black arrows) on the 330K isentropic surface. The result is that deviations from geostrophic balance due to the acceleration of the flow all tend to point in the direction of the ridge. This suggests that the secondary circulation, caused by jetstreaks, has two implications. One being the convergence of extra air mass in the ridge will tend to increase the isentropic density and therefore lower the PV anomaly (increase the negative anomaly in absolute sense) even further. Furthermore air parcels originating from lower levels, which have ascended due to diabatic heating, can find themselves in a environment where the ageostrophic wind points towards the interior of the ridge. Figure 5.11a shows that the ageostrophic wind at lower levels only seems to describe the cyclostrophic balance, while the ageostrophic wind at 330K definitely shows ageostrophic wind perpendicular to geostrophic motion, pointing into the ridge. This could potentially explain why so many air parcels from the interior of the ridge have a history of latent heat release as found by Pfahl et al. (2015). In addition, this also means there is no reason to assume latent heat release is of the same importance as the advection of low valued PV air. Moreover, this could be a consequence of ageostrophic wind at greater height due to the ageostrophic wind.

Otherwise than the fact that at upper levels an ageostrophic wind blows into the interior of the ridge, there seem to be very few signatures of a distinctive secondary circulation flowing around the jetstreak. Therefore it is doubtful if the secondary circulation in this case study has a significant impact on Rossby wave growth.

(a) 11-03-2020, 12UTC, 315K

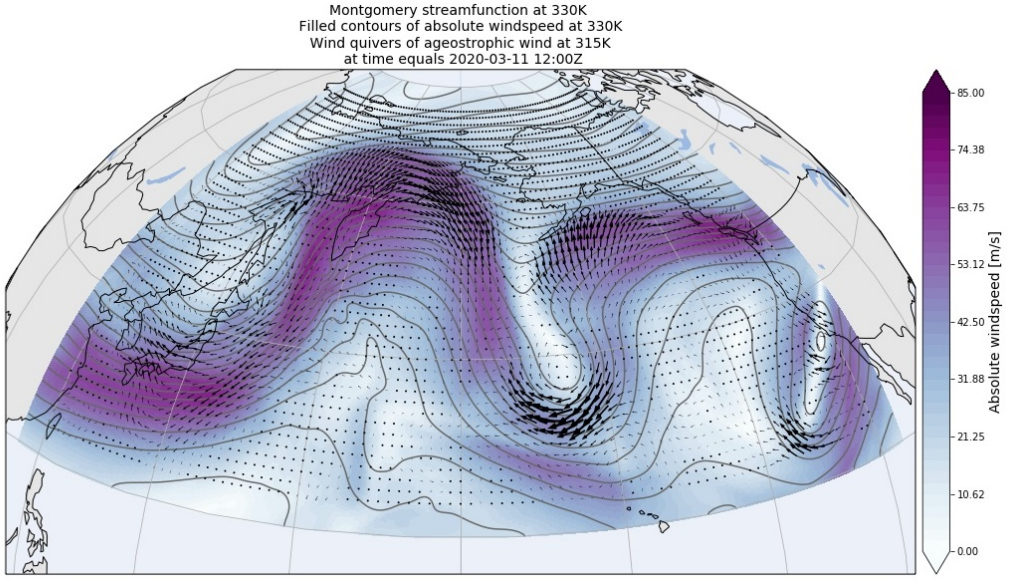

(b) 11-03-2020, 12UTC, 330K

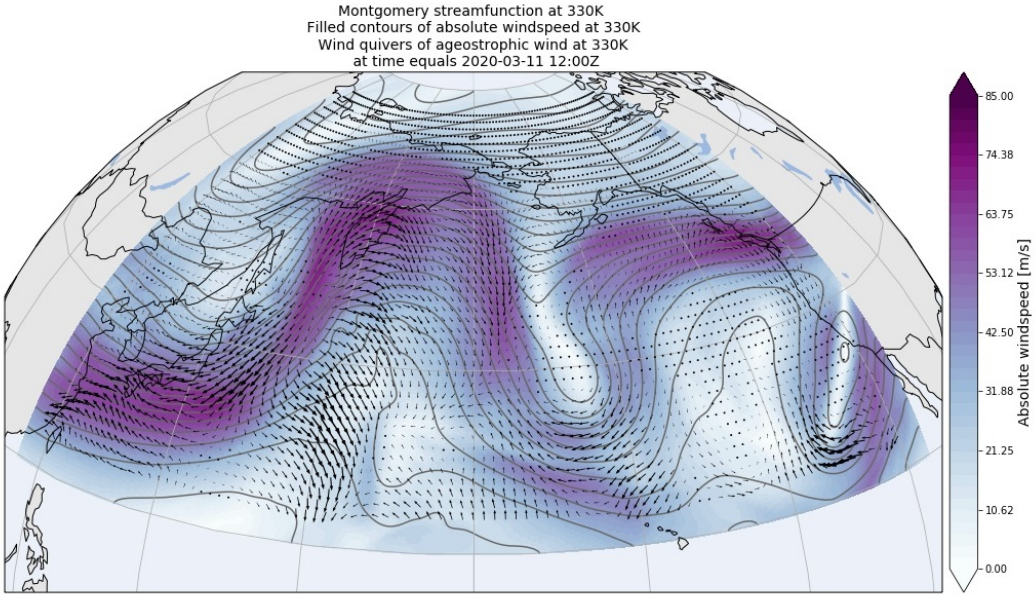

Figure 5.11: Ageostrophic wind (arrows), absolute wind velocity (colours), and Montgomery streamfunction (solid contours) at (a) 315K and (b) 330K.

6

Baroclinic energy conversion in a warming climate

Global warming is obviously one of the main challenges mankind faces in the coming decades, rising sea surface temperatures and accelerating loss of Arctic see ice are undoubtedly consequences of increasing temperatures in the lower atmospheric. The Arctic region has warmed faster than any other region on earth (Serreze and Barry (2011)) and a lot of scientific effort has recently been made on the possibility that this rapid warming impacts weather further south Barnes and Screen (2015). The idea that that mid-latitude extreme weather becomes more common due to polar amplification is widely adopted and publicized by popular news outlets. As explained in this thesis, the mid-latitude jet encapsulates the large scale atmospheric circulation and plays a dominant role in the onset and propagation of synoptic weather events. The fact that the mid-latitude jetstream and mid-latitude weather are undoubtedly coupled, implies that an increase in extreme weather should be accompanied by changing mid-latitude jetstream behaviour.

In this chapter a brief sketch of the qualitative predictions on future temperature trends and the specific implications of this work on mid-latitude jetstream behaviour will be given.

6.1. Model disagreement

The causal relationship between increasing temperatures and the frequency of extreme weather events is perhaps not as clearly straightforward as often suggested in popular science.

However, this link between increasing temperatures and extreme weather scenario's may not be as trivial as one would believe by reading news articles. The effect of increasing temperature on the jetstream is not yet properly elucidated, which makes any predictions about its role in propagating extreme weather events futile. Observational and reanalysis data are not very suitable for studying such connections, because they may include a large amount of internal variability and isolating one effect such as Arctic amplification becomes nigh on impossible. Model simulations offer a viable alternative to study such relationships, because one can force the model in every way possible, and thus isolate certain effects. Cohen et al. (2014) found that almost all experiments with state-of-the-art Atmospheric General Circulation Models (AGCM's) show a causal relation between Arctic warming and the mid-latitude circulation. However the extent and even direction of the response in different models varies wildly with some model experiments showing positive, neutral and negative North Atlantic Oscillation[1,2] (NAO) responses to the forcing of Arctic amplification. This emphasizes that jetstream response to Arctic warming is probably extremely non-linear. Furthermore, it in-

[1]A measure for the meandering pattern of the jetstream. The positive NAO phase corresponds to a strong zonal jetstream, while a negative phase can result in a more meandering pattern.
[2]Also Arctic Oscillation

dicates that the current knowledge about the jetstream is incomplete and that linkages between extreme weather and Arctic warming have to be made with extreme caution, since the underlying processes are not well understood.

Much debate has been generated by the work of (Francis and Vavrus (2012)), in which evidence is presented that Arctic warming is responsible for increased extreme weather in the mid-latitudes. They argue that Arctic amplification slows down the eastward progression of Rossby waves in the upper-level flow by two processes, namely, weakened zonal winds and increased wave amplitude. Critiscism of this work includes (Barnes (2013)), who argue that the presented results appear to be unsupported by observations, and (Screen and Simmonds (2013)) who state that the outcome of the study is highly dependent on the chosen method and the results are therefore biased.

The discussion regarding the response of jetstream behavior to Arctic amplification is far from settled. Moreover, it is far from certain that jetstream behaviour is currently changing at all.Observed changes in jetstream behaviour, on the timescale of both years and decades, can still very viably be attributed to internal mid-latitude variability Barnes and Screen (2015).

6.2. Influence of baroclinic energy conversion

A quantitative and extensive discussion of the effect of a warming climate on weather events is out of the scope of this chapter and study as a whole. However, qualitatively remarks can be made on the effect of a warmer atmosphere, as currently observed and predicted for the future, on BEC.

As stated before, the lower troposphere in the Arctic region is the fastest warming region on earth, this phenomenon is known as Arctic amplification. The temperature gradient between the equator and the pole is the main driver for the jetstream through the vertical integrated thermal wind. Arctic amplification is reducing the meridional temperature gradient and therefore weakens the jetstream. On the other hand, the opposite happens in the upper troposphere. The tropics warm faster than the poles, thereby increasing the meridional temperature gradient and the integrated vertical thermal wind. This means that currently two opposing effects are acting on the jetstream and it is hard to predict which process becomes dominant in the future. Since the start of satellite observations there is no proof that the jetstream weakens or strengthens. Therefore Lee et al. (2019b) reason that it is more interesting to look at wind shear instead of absolute wind speeds and it has been concluded that although the absolute wind speed has not significantly changed throughout the past decades, the vertical wind shear has increased since 1989 by 15%. This substantiates the claim that upper level meridional temperature gradients are increasing relative to lower levels. This also has some profound effects on the slopes of isentropic surfaces which in turn play a major role in BEC. Slopes of isentropic surfaces at lower levels are decreasing while slopes at upper levels have to increase. Increased slopes mean that there is more APE which can be converted into KE. The result is that at upper-levels there is more energy available to be converted through the process of BEC. On the other hand, BEC at lower levels is expected to decrease.
Following the results of this study, the strength and occurrence of jetstreaks is expected to increase, if the jetstream has a meridional direction. The author therefore expects that it is feasible that amplified Rossby waves may become more common in future climates through the increase of energy generated by BEC. A formal proof of this hypothesis might be out of reach at the moment.

7

Conclusions

The topic of growing and breaking Rossby waves causes a lot of debate within the scientific community and the discussion is far from settled. Different opinions on mid-latitude weather in a warming climate are substantiated by model experiments which are found to be sometimes contradictory (Barnes and Screen (2015). Fundamentally, this discussion is based on the Rossby wave and jetstream behaviour, since these are the main drivers for mid-latitude synoptic weather events. Although there is consensus that Rossby wave are baroclinic, and that dynamical and baroclinic instabilities are necessary for Rossby wave growth, these processes are highly nonlinear which is probably one of the main reasons that this subject is not yet fully understood.

Green (Green (1979)) described baroclinic instability qualitatively on the basis of the slope under which air parcels move. When this slope is less than the slope of the isentropic surface, available potential energy(APE) can be converted into kinetic energy(KE). This principle is used multiple times in the scientific community for the analysis of cyclogenisis, and this thesis continues on such previous work. With the recently released ERA-5 reanalysis spatial and temporal derivatives can be calculated far more accurately then before, which gives an enormous amount of possibilities in atmospheric dynamics. In this thesis, ERA-5 is used for studying the principle of baroclinic instability as introduced by Green. An efficiency is introduced for quantifying this so-called ***baroclinic energy conversion***(BEC). It was argued that the amount of baroclinic energy conversion, if it fulfills the instability criteria, depends on the vertical velocity of the air parcel and the slope relative to the isentropes.

It is found that BEC is a very dynamical process substantiated by the fact that areas of BEC are constantly moving through the atmosphere. This implies that the energy source for BEC is indeed the slope of the isentropes and that when this energy is converted, the isentropes flatten and the potential for BEC diminishes until the isentropic gradient is restored. This is in line with previous work from Papritz and Spengler (2015). Furthermore, from mapping the efficiency term is has become clear that although regions of BEC are not equally intense in different locations, it occurs in throughout a multitude of different regions of the atmosphere. This indicates that even when vertical velocities are small, in many cases APE still gets converted into KE. One could think of this as the atmosphere is constantly 'trying' to be in a state of minimal APE, which would be in line with model experiments from O'Gorman and Schneider (2008), where the authors found that changes in kinetic energy approximately scale linearly with the available potential energy averaged over the baroclinic zone.

Baroclinic energy conversion depends on vertical velocities and hence the most intense regions of BEC are found to coincide with regions of large vertical velocities. In the case study these regions are mainly present in the vicinity of relative vorticity maxima and minima where the main flow is still largely meridional. From the theory it is evident that large amounts of APE get converted into KE in these areas and that consequently the main flow has

to accelerate. To see this correlation, BEC and absolute wind speed are mapped in the same figure. In an Eulerian frame it was striking that jetstreaks coincide with intense regions of BEC, meaning that BEC could be the driver for formation or strengthening of jetstreaks. In turn, jetstreaks could steer the jetstream in the meridional direction and therefore amplify Rossby waves. Furthermore, accelerations of the main flow have be accompanied by deviations from geostrophic balance. At higher levels, these deviations have a wind velocity contribution perpendicular to the geostrophic flow which point into the ridge. This can therefore increase the isentropic density, which would lower the PV anomaly in the case study. However, a very distinctive secondary ageostrophic circulation is not found and the importance of the ageostrophic wind to Rossby wave amplification is not presented with a lot of certainty.

A Lagrangian framework was build to further investigate the link between BEC and jetstreaks. Twenty air parcels were followed on the 330K isentropic level while moving through a distinctive area of intense unstable upgliding. The correlation between BEC and absolute wind velocity and between BEC and wind accelerations both indicate that when BEC is intense, air parcels have in general higher absolute wind velocities and a higher change to be accelerated. However, both results were characterized by a lot of variability, such that fitting a trend was impossible. Therefore it is hard to make robust claims about the relation between BEC and jetstreaks.

Further research could focus on using the theory of baroclinic energy conversion and testing it in multiple cases of Rossby wave amplification or breaking, to find more robust patterns between BEC and jetstreaks. Furthermore, deviations from geostrophic balance do not show a distinctive secondary circulation, further research could also focus on the response of the atmosphere to accelerations.

A

Code

Much of this thesis depends on the code I wrote in Python. The used code (and more) will be made available at GitHub, so that further research on baroclinic energy conversion could make use of the code I wrote, when this is helpful.

Bibliography

Elizabeth A. Barnes. Revisiting the evidence linking Arctic amplification to extreme weather in midlatitudes. ***Geophysical Research Letters***, 40(17):4734–4739, 2013. ISSN 00948276. doi: 10.1002/grl.50880.

Elizabeth A. Barnes and James A. Screen. The impact of Arctic warming on the midlatitude jet-stream: Can it? Has it? Will it? ***Wiley Interdisciplinary Reviews: Climate Change***, 6(3): 277–286, 5 2015. ISSN 17577799. doi: 10.1002/wcc.337.

Judah Cohen, James A. Screen, Jason C. Furtado, Mathew Barlow, David Whittleston, Dim Coumou, Jennifer Francis, Klaus Dethloff, Dara Entekhabi, James Overland, and Justin Jones. Recent Arctic amplification and extreme mid-latitude weather, 2014. ISSN 17520908.

P. Davini, C. Cagnazzo, and J. A. Anstey. A blocking view of the stratosphere-troposphere coupling. ***Journal of Geophysical Research***, 119(19):100–11, 10 2014. ISSN 21562202. doi: 10.1002/2014JD021703.

Aarnout Van Delden. The slope of isentropes constituting a frontal zone. ***Tellus A: Dynamic Meteorology and Oceanography***, 51(5):603–611, 1 1999. doi: 10.3402/tellusa.v51i5.14479.

Jennifer A. Francis and Stephen J. Vavrus. Evidence linking Arctic amplification to extreme weather in mid-latitudes. ***Geophysical Research Letters***, 39(6), 3 2012. ISSN 00948276. doi: 10.1029/2012GL051000.

J S A Green. TOPICS IN DYNAMICAL METEOROLOGY: 8. TROUGH-RIDGE SYSTEMS AS SLANTWISE CONVECTION (1). ***Weather***, 34(1):2–10, 1979. doi: 10.1002/j.1477-8696.1979.tb03366.x. URL `https://rmets.onlinelibrary.wiley.com/doi/abs/10.1002/j.1477-8696.1979.tb03366.x`.

James R Holton and Gregory J Hakim. Chapter 2 - Basic Conservation Laws. In James R Holton and Gregory J Hakim, editors, ***An Introduction to Dynamic Meteorology (Fifth Edition)***, pages 31 – 66. Academic Press, Boston, fifth edition edition, 2013. ISBN 978-0-12-384866-6. doi: https://doi.org/10.1016/B978-0-12-384866-6.00002-7. URL `http://www.sciencedirect.com/science/article/pii/B9780123848666000027`.

B J Hoskins', M E Mcintyre', and A W Robertson3. On the use and significance of isentropic potential vorticity maps. Technical report, 1985.

H. Joos and H. Wernli. Influence of microphysical processes on the potential vorticity development in a warm conveyor belt: A case-study with the limited-area model COSMO. ***Quarterly Journal of the Royal Meteorological Society***, 138(663):407–418, 1 2012. ISSN 00359009. doi: 10.1002/qj.934.

Kai Kornhuber, Dim Coumou, Elisabeth Vogel, Corey Lesk, Jonathan F. Donges, Jascha Lehmann, and Radley M. Horton. Amplified Rossby waves enhance risk of concurrent heatwaves in major breadbasket regions, 1 2020. ISSN 17586798.

S. H. Lee, A. J. Charlton-Perez, J. C. Furtado, and S. J. Woolnough. Abrupt Stratospheric Vortex Weakening Associated With North Atlantic Anticyclonic Wave Breaking. ***Journal of Geophysical Research: Atmospheres***, 124(15):8563–8575, 2019a. ISSN 21698996. doi: 10.1029/2019JD030940.

Simon H. Lee, Paul D. Williams, and Thomas H.A. Frame. Increased shear in the North Atlantic upper-level jet stream over the past four decades. ***Nature***, 572(7771):639–642, 8 2019b. ISSN 14764687. doi: 10.1038/s41586-019-1465-z.

Edward N Lorenz. Available Potential Energy and the Maintenance of the General Circulation. Technical report.

Noboru Nakamura and Clare S Y Huang. Atmospheric blocking as a traffic jam in the jet stream. Technical report. URL http://science.sciencemag.org/.

Thando Ndarana and Darryn W. Waugh. The link between cut-off lows and Rossby wave breaking in the Southern Hemisphere. *Quarterly Journal of the Royal Meteorological Society*, 136(649):869–885, 4 2010. ISSN 00359009. doi: 10.1002/qj.627.

Paul A. O'Gorman and Tapio Schneider. Energy of midlatitude transient eddies in idealized simulations of changed climates. *Journal of Climate*, 21(22):5797–5806, 2008. ISSN 08948755. doi: 10.1175/2008JCLI2099.1.

Lukas Papritz and Sebastian Schemm. Development of an idealised downstream cyclone: Eulerian and lagrangian perspective on the kinetic energy. *Tellus, Series A: Dynamic Meteorology and Oceanography*, 65, 2013. ISSN 16000870. doi: 10.3402/tellusa.v65i0.19539.

Lukas Papritz and Thomas Spengler. Analysis of the slope of isentropic surfaces and its tendencies over the North Atlantic. *Quarterly Journal of the Royal Meteorological Society*, 141 (693):3226–3238, 10 2015. ISSN 1477870X. doi: 10.1002/qj.2605.

J L Pelly and B J Hoskins. A New Perspective on Blocking. Technical report, 2003.

S. Pfahl, C. Schwierz, M. Croci-Maspoli, C. M. Grams, and H. Wernli. Importance of latent heat release in ascending air streams for atmospheric blocking. *Nature Geoscience*, 8(8): 610–614, 8 2015. ISSN 17520908. doi: 10.1038/ngeo2487.

N. Schaller, J. Sillmann, J. Anstey, E. M. Fischer, C. M. Grams, and S. Russo. Influence of blocking on Northern European and Western Russian heatwaves in large climate model ensembles. *Environmental Research Letters*, 13(5), 5 2018. ISSN 17489326. doi: 10.1088/1748-9326/aaba55.

James A. Screen and Ian Simmonds. Exploring links between Arctic amplification and midlatitude weather. *Geophysical Research Letters*, 40(5):959–964, 3 2013. ISSN 00948276. doi: 10.1002/grl.50174.

Mark C. Serreze and Roger G. Barry. Processes and impacts of Arctic amplification: A research synthesis. *Global and Planetary Change*, 77(1-2):85–96, 5 2011. ISSN 09218181. doi: 10.1016/j.gloplacha.2011.03.004.

Alan J Thorpe. An appreciation of the meteorological research of Ernst Kleinschmidt. Technical report, 1993.

Aarnout van Delden and Roel Neggers. A case study of tropopause cyclogenesis. *Meteorological Applications*, 10(2):187–199, 6 2003. ISSN 13504827. doi: 10.1017/S1350482703002081.

Chris Weijenborg, Hylke de Vries, and Reindert J. Haarsma. On the direction of Rossby wave breaking in blocking. *Climate Dynamics*, 39(12):2823–2831, 11 2012. ISSN 09307575. doi: 10.1007/s00382-012-1332-1.

Tim Woollings, Abdel Hannachi, and Brian Hoskins. Variability of the North Atlantic eddy-driven jet stream. *Quarterly Journal of the Royal Meteorological Society*, 136(649):856–868, 4 2010. ISSN 00359009. doi: 10.1002/qj.625.

Tim Woollings, David Barriopedro, John Methven, Seok Woo Son, Olivia Martius, Ben Harvey, Jana Sillmann, Anthony R. Lupo, and Sonia Seneviratne. Blocking and its Response to Climate Change, 9 2018. ISSN 21986061.

Akira Yamazaki Dr. and Hisanori Itoh. Vortex-vortex interactions for the maintenance of blocking. part I: The selective absorption mechanism and a case study. *Journal of the Atmospheric Sciences*, 70(3):725–742, 3 2013. ISSN 00224928. doi: 10.1175/JAS-D-11-0295.1.